frontiers | Frontiers in Aquaculture

TYPE Original Research
PUBLISHED 18 October 2024
DOI 10.3389/faquc.2024.1388280

OPEN ACCESS

EDITED BY
Tiago Hori,
Atlantic Aqua Farms Ltd, Canada

REVIEWED BY
Mario Oertel,
Helmut Schmidt University, Germany
Sulaiman Olanrewaju Oladokun,
Universiti Malaysia Perlis, Malaysia

*CORRESPONDENCE
Nils Goseberg
n.goseberg@tu-braunschweig.de

RECEIVED 19 February 2024
ACCEPTED 12 September 2024
PUBLISHED 18 October 2024

CITATION
Lojek O, Goseberg N, Føre HM, Dewhurst T, Bölker T, Heasman KG, Buck BH, Fredriksson DW and Rickerich S (2024) Hydrodynamic exposure – on the quest to deriving quantitative metrics for mariculture sites.
Front. Aquac. 3:1388280.
doi: 10.3389/faquc.2024.1388280

Hydrodynamic exposure – on the quest to deriving quantitative metrics for mariculture sites

Oliver Lojek[1], Nils Goseberg[1,2]*, Heidi Moe Føre[3], Tobias Dewhurst[4], Thea Bölker[1], Kevin Gerald Heasman[5], Bela H. Buck[6,7], David W. Fredriksson[8] and Samuel Rickerich[4]

[1]Department of Hydromechanics, Coastal- and Ocean Engineering, Leichtweiß-Institute for Hydraulic Engineering and Water Resources, Technische Universität Braunschweig, Braunschweig, Germany, [2]Coastal Research Center, Joint Research Facility of Technische Universität Braunschweig and Leibniz Universität Hannover, Hannover, Germany, [3]Department of Energy and Transport, SINTEF Ocean, Trondheim, Norway, [4]Kelson Marine Co., Portland, ME, United States, [5]Blue Technology Group, Cawthron Institute, Nelson, New Zealand, [6]Marine Aquaculture, Alfred Wegener Institute Helmholtz Centre for Polar and Marine Research (AWI), Bremerhaven, Germany, [7]Applied Marine Biology, University of Applied Sciences Bremerhaven, Bremerhaven, Germany, [8]Center for Sustainable Seafood Systems, University of New Hampshire, Durham, NH, United States

This work attempts to define metrics for hydrodynamic exposure, using known oceanographic variables to provide a universal site assessment method for mariculture structures. Understanding environmental conditions driving open-ocean mariculture siting is crucial in establishing consistent ocean governance, minimizing adverse environmental impacts, and facilitating economically sustainable farm operations. To provide a metric of oceanic conditions and associated requirements for structural design and operation of aquaculture systems, six Exposure Indices (EI) are proposed that consider physical energy levels related to hydrodynamic forces at a site. Four of the proposed indices consider only environmental conditions, while the other two also consider the dimensions of the gear that is exposed to the external loads. These indices are: Exposure Velocity (EV), Exposure Velocity at Reference Depth (EVRD), Specific Exposure Energy (SEE), Depth-integrated Energy Flux (DEF), Structure-centered Depth-integrated Energy (SDE), and a Structure-centered Drag-to-Buoyancy Ratio (SDBR). While these indices are derived with a focus on aquaculture structures, they may also have applications for estimating biological stressors and operational challenges. The proposed exposure indices were evaluated for a range of known aquaculture sites around the world. A sensitivity analysis was conducted that quantified the relationship between the exposure indices and storm event return period. At a regional scale, hindcast numerical data for the German Bight combined with calculations of 50-year extreme values were used to calculate and map each proposed index spatially. Resulting maps showed that exposure is not simply a function of distance from shore. The six indices show plausible performance regarding the objective assessment of aquaculture sites. The authors herein present the indices to the aquaculture and ocean engineering communities for discussion, application, and potential adoption of one or more of the proposed indices.

KEYWORDS

aquaculture siting, degree of exposure, hydrodynamic loading, aquaculture technology, aquaculture engineering, quantitative assessment, operation, maintenance

1 Introduction

The United Nations sustainable development goals (SDG) clearly set out the world's ambition to reduce hunger (SDG #2), while simultaneously advocating sustainable production and consumption (SDG #12) (United Nations, 2020; FAO, 2020). As the global population is projected to increase over the next decades to reach 9.8 billion by 2050 and 11.2 billion by 2100 (United Nations, 2022; Chao et al., 2021), so is the demand for food projected to increase in an attempt to reduce hunger and poverty. Low- and middle-income countries have shown a considerable increase in demands for animal proteins (Tilman et al., 2011), in turn driving the dynamics in utilizing formerly unused land or sea plots for farming practices around the globe affecting over 30% of the landmass in just six decades (van Vliet et al., 2015; Winkler et al., 2021). Poore and Nemecek (2018) indicate that the production of animal protein has a disproportionally higher environmental impact per calorie than plant-based proteins. Foods farmed in aquatic water bodies have far lower carbon footprints (CF) than land-based production of protein (MacLeod et al., 2020). Large seaweed farms have the potential to sequestrate carbon efficiently (Krause-Jensen and Duarte, 2016), though the economics are still challenging (Coleman et al., 2022a, 2022b; Sulaiman and Abdul Raship, 2013). Salmon farming studies in various countries reaffirm that the CF of most aquaculture systems is lower than the footprint of any other form of animal protein production systems (Nijdam et al., 2012; MacLeod et al., 2020), the largest part being production and transport of feed. Mariculture hence appears to be a very promising alternative to land-based food production (Costa-Pierce et al., 2021; Costa-Pierce, 2016). Recent technological developments in allowing mariculture production in more exposed conditions indicate opportunities to further minimize CF while improving productivity (Boyd et al., 2020). Examples of novel production systems or new concepts bringing aquaculture into more exposed waters are the shellfish tower (Heasman et al., 2021; Landmann et al., 2021), multi-use concepts (Buck et al., 2004), shellfish longlines (Stevens et al., 2008; Goseberg et al., 2017 or open ocean fish cage systems (Moe Føre et al., 2022; Fredriksson et al., 2004).

Understanding the potential for, and the conditions driving mariculture siting, is crucial in establishing sustainable ocean governance, minimizing environmental impact, and facilitating economically sustainable farm operations. A recent mapping study by Clawson et al. (2022) has provided a database for existing and potential mariculture sites at a global scale. In absence of more accurate information, siting potential has been defined by criteria such as distance from port and from coast as well as number of known sites; their siting algorithm then was validated based on known aquaculture sites. However, this approach is not taking into account site-specific oceanographic conditions which in real mariculture operations often supersede mere distance-based criteria. Therefore, a need exists to define and eventually establish an exposure index (EI) that represents both oceanic conditions and associated requirements for structural design and operation of aquaculture systems. Such an index would assist potential farmers, equipment developers, policy developers, regulators, and insurers alike. In the past, such a definition has been difficult to determine due to the multitude of unassociated users with different needs. Oceanic exposure is notoriously difficult to describe and hence various terms touch on these conditions, e.g. 'offshore', 'nearshore', 'sheltered' or 'exposed' (cp. also Froehlich et al., 2017). These terms are used to help characterize the site-specific level of engineering required to ensure structural mariculture system integrity. In Buck et al. (2024), considerable variations and ambiguities in the definitions of offshore aquaculture were found, but all implied distance from shore. The authors agree, however, that it is not the distance from the coast but primarily the exposure to waves and currents that is the more important factor in classification of an aquaculture site.

This work consequently attempts to define a set of metrics for hydrodynamic exposure, using standard oceanographic variables to provide a universally valid site assessment method for mariculture structures. These possible indices we present are essentially considering physical energy levels or hydrodynamic forces at a site, with a two-pronged view: a first view is purely considering external loads while a second view is additionally considering the dimensions of the gear that is exposed to the external loads. An EI provides a quantified continuum of increasing environmental intensity (and resultant energy tolerant structures and considerations) with increasing exposure. The rationale behind the EI is that the intensity of the hydrodynamic conditions at a site will dictate or heavily impact: the equipment required; the species that can be cultivated at the site; the vessels required to service the site and species; the operation and maintenance methods; the logistics including management/frequency of delivery of feeds (if finfish); aspects of the environmental impacts; the degree of risk mitigation required (to the farmer, the environment, to the financier and to the insurer). Quantifying these parameters in a single metric will assist regulators to issue permits/licenses, assist developers in selecting gear types, assist farmers in considering operational logistics, and generally be useful to all investigators. A suitably defined EI will also help to fill in data gaps for and about mariculture identified by Froehlich et al. (2022), as such indices would provide spatial information about farming potential that can be directly used in digital assessment systems.

Three primary factors, which influence the intensity of a site, were identified in Buck et al. (2024): Waves (height and period/length), ocean currents (speed) and water depth. It is understood that there are variables within these primary factors such as the depth-variable current profile that also influence levels of energy. To accommodate such natural variations and investigate the usefulness of a range of approaches, a number of methods to describe exposure were developed. All are potentially useful, but they emphasize different considerations and exhibit varying degrees of sensitivity. The authors acknowledge that no single method exists that considers all fluctuations, variations and nuances. However, quantifying various index results may yield insightful information to investors, insurers, businesses, ventures, and regulators. Normalized results readily render multiple facets of aquatic site conditions assessable with one standardized metric. This will enable stakeholders to gain a sophisticated perspective on the suitability

and limitations of a potential aquaculture site. The benefit of the EI is that it combines the numerous independent environmental factors into a single generally applicable metric.

More specifically, the work which overall aims to quantitatively describe hydrodynamic exposure of mariculture sites has the following objectives:

- To provide a broad perspective on potential formulations of hydrodynamic exposure and lay out their basic meaning.
- To apply the formulated indices to known aquaculture sites worldwide to compare their exposure on a global scale.
- To map the indices to understand spatial variations on a basin scale.
- To provide a thorough discussion on advantages and disadvantages of the suggested hydrodynamic exposure indices.

The remainder of this work is organized as follows: Section 2 gives an overview of the various developed EIs, explains the normalization across the indices and introduces oceanographic data used. Section 3 showcases exemplary results obtained with different EIs for select sites around the globe as well as a high-resolution index map of the North Sea. Section 4 discusses the advantages and disadvantages of the introduced EIs, while Section 5 draws a conclusion and gives an outlook of work to do.

2 Materials and methods

2.1 Quantitative metrics to measure hydrodynamic exposure

In the design of aquaculture structures, perhaps the most critical component of the process is the quantification of the environmental parameters specific to a potential mariculture site, which are usually summarized in a site selection criteria catalogue (Aguilar-Manjarrez et al., 2017; Benetti et al., 2010; Gentry et al., 2017; Helsley, 1997; Oyinlola et al., 2018; Longdill et al., 2008; Kapetsky et al., 2013; Buck and Grote, 2018). From the land-dwelling, human perspective, it may be natural to define a site by distance from shore. Of course, distance is relevant for the operation of aquaculture farms, but it is not the primary factor governing exposure to environmental loads. Therefore, from the ocean engineering viewpoint, it is logical to define the location by the magnitude of interaction between the ocean environment and the aquaculture structure. The intensity of oceanographic conditions, typically in the form of waves and currents, impose forces on the aquaculture structures which generally increase with increasing fluid velocities and accelerations. Wind loads should also be considered in structural design, but wave and current loads generally dominate because most aquaculture structures have considerably more volume below the waterline than above. The dimensions of aquaculture system components, range from small diameter twine (millimeters) (Loverich and Forster, 2000; Loverich and Gace, 1997; Føre et al., 2022) of fish containment net to farms that cover hectares of sea area (Gray, 2019; Goseberg et al., 2017). Aquaculture system components are often the products themselves composing of shellfish droppers or thickly grown macroalgae with scales from one to 100s of meters (Chopin and Sawhney, 2009).

The approach described here considers the relative size of individual aquaculture system components to distinguish it from other "offshore" industry structures used for oil/gas, wind and hydrokinetics. This was done to identify the relevant types of forces (drag/inertia) and therefore the variables used in the development of the index.

2.1.1 Definition of variables to formulate exposure indices

The parameters that have been identified as the dominant parameters of the hydrodynamic energy at the aquatic site are: significant wave height (H_s), peak wave period (T_p), water current speed (U_c), wave induced current or orbital velocity (u) in the horizontal direction, and the depth of water at a site (d). Here, the current speed is the complement to the wave induced orbital velocity; U_c encompasses currents driven by tides, winds, buoyancy, and wave-driven mean flows while u is only the orbital velocity. By considering these environmental characteristics, several mathematical formulations were considered. It is important to note that *EI*s require that the hydrodynamic parameters of the site under consideration must be known (either from measurements or numerical modeling) to inform the index calculation. Since waves attenuate and current velocities can vary with depth, both are a function of vertical position in the water column (z). The corresponding hydrodynamic loads acting on the aquaculture structure may change with submergence at the same site due to decreased wave-induced fluid velocities (u_w) as shown on Figure 1.

The exposure index must also be defined according to a desired probability function and return period (e.g., 50-year storm condition). These parameters can be obtained from model results, field datasets, hind-/forecasts or other acceptable methods. Once this condition has been identified, the corresponding design values for H_s, T_p, and depth-dependent U_c can be determined for a site. For instance, with the wave period and depth, the wavelength (L) can be defined with linear wave theory (e.g. Dean and Dalrymple, 1991; USACE, 2002), by the dispersion relation:

$$L = \frac{gT_p^2}{2\pi} tanh(kd) \tag{1}$$

with g being the gravitational acceleration and where k is the wave number:

$$k = \frac{2\pi}{L} \tag{2}$$

The dispersion relation requires a numerical solution to obtain the wavelength, as a function of depth at the site, since it is found both inside and outside of the hyperbolic tangent function. With the wavelength, the relative depth is defined as:

$$Relative\ \ Depth = \frac{d}{L}. \tag{3}$$

As a wave propagates from deep to shallow water the wave period remains constant, but the wavelength decreases and

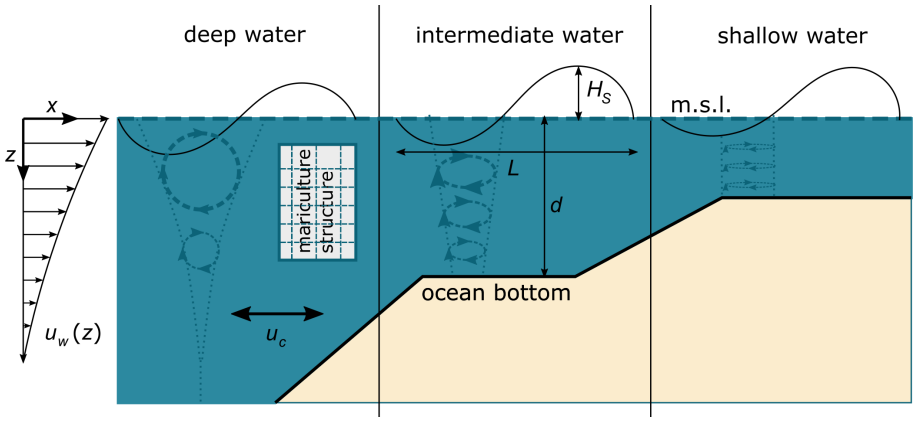

FIGURE 1
Waves and currents are site specific with parameters a function of vertical location in the water column (z). As waves propagate from deep to shallow water, wave height and length change as a function of (x).

therefore the wave heights shoal (increase) until they become steep enough to break. For a fixed wave period, increasing wave heights increase the horizontal wave velocities (u) and accelerations (du/dt, t time) and the forces on the structure.

Wave and current forces on aquaculture structures that consist of cylinders with a diameter (D) can be approximately calculated using a per unit length form of Morison's equation (Morison et al., 1950):

$$f_x = C_D D \frac{1}{2} \rho (u + U_c)|u + U_c| + C_m \rho \frac{\pi D^2}{4} \frac{\partial u}{\partial t} \quad (4)$$

assuming that the size of diameter (D) is small compared to the wavelength (L). In Equation 4, C_D is the drag coefficient, ρ is the mass density of the fluid, C_m is the mass coefficient and u is the instantaneous horizontal wave particle velocity:

$$u(x, z, t) = \frac{\pi H}{T} \frac{\cosh k(z + d)}{\sinh (kd)} cos(kx - \omega t) \quad (5)$$

The horizontal wave particle velocity oscillates as a function of the cosine term and therefore in Equation 5 the absolute value sign maintains the direction of u. The magnitude of the wave-induced fluid velocity can be written as:

$$u_w(z) = \frac{\pi H}{T} \frac{\cosh k(z + d)}{\sinh (kd)}, \quad (6)$$

showing attenuation with vertical position in the water column (z). The velocity term in Equation 4 also includes a steady component, $U_c(z)$, also shown on Figure 1. Aside from the depth-dependent velocity induced by waves when acting on a slender cylindrical body, as shown in Equation 4, acceleration components also exist. These acceleration-dependent forces, related to the inertia of the water oscillating around the cylinder, are represented by the function of $\frac{\partial u}{\partial t}$. The dominance of wave drag over wave inertia forcing on a structure is characterized by the Keulegan-Carpenter number (Keulegan and Carpenter, 1958) expressed as:

$$KC = \frac{u \cdot T_P}{D} \quad (7)$$

The KC number is typically calculated using particle orbital velocities u (Sarpkaya, 2014).

As discussed in McCormick (2010), (wave) drag dominates for small diameter cylinders if the KC number is on the order of 100, which could represent a KC number threshold. This would be the case if $u_w = 1 \frac{\text{m}}{\text{s}}$, $T_p = 10$ s and $D = 0.1$ m. Inertia force dominance would increase as the submerged diameter (or volume) of the structure becomes larger, decreasing KC to level of ≈ 10. In this context, it is assumed that aquaculture structures like mussel droppers, kelp-lines, rope, net and buoys are all slender as compared to wave height H_s and length L. The drag dominance would increase the wave velocities is combined with the steady current velocities.

2.1.2 Hydrodynamic exposure indices

This work proposes and examines six hydrodynamic exposure indices that are based on the variable definitions described in Equation 8 to Equation 19. The first four indices were developed based on the environmental loading variables wave length, water depth, wave- and current-induced velocities, while the fifth and sixth index also include geometric and other characteristic information of some aquaculture technology, such as the structure's diameter. The indices take as input the defined hydrodynamic oceanographic variables, all of which are typically derived using extreme value analysis based on measurements or hind-cast simulations. Therefore, when using the indices, it is important to recognize that these values are probabilistic by nature. Input variables should generally be design values, e.g., using return periods (occurrences) of 50 years. The following candidate indices are proposed and examined:

1. Exposure Velocity (EV)
2. Exposure Velocity at Reference Depth (EVRD)
3. Specific Exposure Energy (SEE)
4. Depth-integrated Energy Flux (DEF)
5. Structure-centered Depth-integrated Energy (SDE)
6. Structure-centered Drag-to-Buoyancy Ratio (SDBR)

The benefits, challenges and specific reasoning in defining each index are presented next.

2.1.2.1 Exposure velocity

Drag forces on aquaculture structures in oceanic conditions are strongly tied to the combined current- and wave-induced velocity field at some depth measured from the sea surface. In accordance with Equation 5, the total fluid velocity takes into account the depth-dependent orbital velocities (see Figure 1) and the water currents; the latter are typically an intricate state of e.g., tidal and circulation oceanic currents. This definition of exposure velocity incorporates the nonlinear wave-current interaction. That is,

$$Exposure\ \ Velocity\ \ (EV) = \sqrt{u_w(z)^2 + 2u_w(z)U_c(z) + \ U_c(z)^2} = U_c(z) + u_w(z) \quad (8)$$

Equation 9 can be applied for a given depth, wave height, wave period and position in the water column. Where not otherwise specified, the analyses presented here surface values, which generally correspond to the highest exposure level over the water depth.

2.1.2.2 Exposure velocity at reference depth

Aquaculture structures can be deployed at various depths below the water surface. Many extend down from near the surface such as seaweed (extending 0 - 10 m) and mussel farming lines (extending 0 - 20 m) or fish nets (extending 20 - 50 m) (Heasman et al., 2021; Stevens et al., 2008). In addition, submerged structures may become highly relevant in exposed sites. To achieve a common measure of exposure velocity for a specific site independent of types of structures, a reference depth of 10 m has been proposed for this special case of the EV index. Considering a structure with a depth of 10 m, the suggested exposure velocity is given as the average horizontal current velocity plus the average maximum particle velocity over this depth in a given direction. To simplify further (avoiding integration over a certain water depth), current velocity design values at 5 m (U_{c5}) and the horizontal particle velocity (Equation 5) at 5 m (u=u_{w5_max}) is assumed to represent the average current and wave particle velocities respectively over the reference depth. This gives the following mathematical expression of the Exposure Velocity at Reference Depth (EVRD):

$$Exposure\ \ Velocity\ \ at\ \ Reference\ \ Depth\ \ (EVRD) = \ U_E = U_{c5} + u_{w5} \quad (9)$$

where the indices 'c' and 'w' represent the current- and wave-induced velocities, respectively. Alternative depth definitions are possible, when applied to actual mariculture operations.

2.1.2.3 Specific exposure energy

The intensity of extreme conditions at aquaculture sites may be related to the energy in the moving seawater. For a moving mass of uniform fluid, the kinetic energy can be described as,

$$E = \frac{1}{2}\ m\ \ U^2 \quad (10)$$

where m is the mass of fluid and U is its instantaneous velocity. Current and wave-induced fluid velocities can be incorporated by defining U as the exposure velocity derived above, which is the sum of a steady and a wave-induced fluid velocity for the point of interest,

$$U(z) \ = \ U_c(z) \ + \ u_w(z) \quad (11)$$

Dividing kinetic energy by m yields kinetic energy per unit mass, which can be described as the *Specific Exposure Energy (SEE)*. That is,

$$\text{Specific Exposure Energy (SEE)} = \ 1/2 \ \ (U_c(z) \ + \ u_w(z))^2 \quad (12)$$

This index has SI units of J/kg. Since drag force on any gear is nominally proportional to fluid velocity squared, drag forces will also be proportional to the Specific Exposure Energy.

This exposure index can also be extended to a structure-centric index by multiplying a site's SEE (e.g., in J/kg) by the mass of the displacement water of the aquaculture structure (in kg), to yield a structure-centric exposure energy with SI units of Joules.

2.1.2.4 Depth-integrated energy flux

Another proposed quantitative metric is called the energy flux (DEF) index and is the sum of energy flux due to both waves and currents integrated over the water depth. Wave energy flux is equivalent to units of power, and is often quantified in energy flux per unit width (e.g., W/m, in SI). One motivation for using the Specific Exposure Energy, is that it provides a relevant and quantified metric for kinetic energy. Furthermore, wave energy flux at many coastal locations has been quantified and mapped in wave and marine current renewable energy production (Drew et al., 2009; Jin et al., 2022). For deep water waves, the wave energy flux (power) per unit width, W/m, due to wave action in a given sea state is defined as:

$$Wave-based\ \ Energy\ \ Flux = \frac{\rho g^2 (H_s^2) T_E}{64\pi} \quad (13)$$

In Equation 13, T_E is the 'energy period' of the sea state in seconds. For simplicity, the energy period can be estimated to be proportional to the peak period, using the empirical relationship such as $T_E = 0.9T_P$ (c.f., Ahn, 2021). The expression defined here is derived for deep water integrating wave energy flux vertically over the entire water column depth. This technique also incorporates a variance spectrum approach proportional to energy with the use of H_s in m.

The energy flux through a vertical plane normal to the current velocity is proportional to U^3. Integrated over depth, the energy flux per horizontal distance is,

$$Current-based\ \ Energy\ \ Flux\ \ (WEF)_c = \ \frac{1}{2}\rho d (U_c)^3 \quad (14)$$

Thus, a combination of wave- and current-induced energy flux may be approximated by a linear superposition as:

$$Depth-integrated\ \ Energy\ \ Flux\ \ (DEF) = \frac{\rho g^2 (H_s^2) T_E}{64\pi} + \ \frac{1}{2}\rho d (U_c)^3 \quad (15)$$

2.1.2.5 Structure-centered depth-integrated energy

While an environmental loading focus has been the guiding principle for the formulation of the above indices, the authors have opted to include indices that include characteristics related to specific mariculture components, i.e., solidity or a diameter of a hypothetical mariculture structure. Two primary factors in governing total forces of structures are their diameter and the solidity (Gansel et al., 2018, 2015; Føre et al., 2022); To that end, energy content in a unit space of the horizontal ocean domain has been approximated, using basic oceanographic formulations for the energy (in Joule J) that is contained in the water column from the surface elevation to the ocean bottom, integrated horizontally over wavelength. It is comprised of the potential and kinetic wave energy, based on linear wave theory,

$$E_{wave} = \frac{1}{8}\rho g H_s^2. \tag{16}$$

Energy of tidal or oceanic currents can be expressed in terms of kinetic energy per unit area, and may approximately reduce to:

$$E_{current} = \frac{1}{2}\rho d U^2 \quad in \quad [J/m^2]. \tag{17}$$

A simple linear combination the solidity and exposed surface area of a mariculture structure, in our case an idealized cylinder is chosen, with the sum of the wave and current energy can now become an expression for the amount of energy close to a structure, available for wave-current interaction. While higher-order, and non-linear interactions, as well as ratios of drag over inertia forces are neglected in this approach, a simple relation exists that allows to compare simpler mariculture structures independent of location. The structure-centered Depth-integrated Energy index (SDE), using Equation 16 and Equation 17, becomes:

$$Structure-centered\ \ Depth-integrated\ \ Energy\ \ (SDE)$$
$$= \left(\frac{1}{8}gH_s^2 + \frac{1}{2}dU^2\right)\rho S A_{structure} \tag{18}$$

where $S = A_p/A$ defines the solidity of a mariculture structure as the ratio of the area of gear material A_p and the total area covered by a reference area A (Zhan et al., 2006; Tsukrov et al., 2011). In addition, the surface area over which the energy is integrated is $A_{\text{structure}} = \pi \cdot D^2/4$. This index can also be converted to a structure-agnostic index by simply removing the factors S and $A_{\text{structure}}$ *from* Equation 18.

2.1.2.6 Structure-centered drag-to-buoyancy ratio

To achieve an exposure index that is proportional to energy and drag forces and is non-dimensional, an alternative structure-centric index is proposed based on the ratio of drag forces to buoyant forces on an aquaculture structure. In this formulation,

$$Drag-to-buoyancy\ \ Ratio = \frac{Drag\ \ force}{Buoyancy\ \ force}$$
$$= \frac{\frac{1}{2}\rho C_D A U^2}{\rho g V} \tag{19}$$

with U being the exposure velocity as calculated previously ($U = U_c(z) + u_w(z)$). The projected area, A, can be taken to be proportional to D^2 (where, as before, D is the characteristic length associated with the structure). Similarly, volume, V, is proportional to D^3. Taking a representative drag coefficient of $C_D = 1$, the equation above becomes:

$$Drag-to-buoyancy\ \ Ratio\ \ (SDBR) = \frac{U^2}{2gD} \tag{20}$$

This structure-centric index has the benefit of being a non-dimensional number. Note that the parameter D is a characteristics length of a structure, and not the local water depth in which the structure is placed; thus, the SDBR should not be confused with a Froude number squared.

2.2 Oceanographic data and exposure indices for known aquaculture sites

The proposed exposure indices were evaluated for a range of known aquaculture sites around the world. Site parameters including extreme values for wave and current magnitudes were provided via personal communication with members of the International Council for the Exploration of the Seas (ICES) Working Group on Open-Ocean Aquaculture (WGOOA) and collaborators. The derivation of site-specific extreme values is not the focus of this paper. Therefore, the extreme values listed here were accepted as provided and should not be used for design or other purposes.

2.3 Oceanographic data and exposure indices at the regional scale

2.3.1 Database EasyGSH for the German Bight North Sea

A wide range of applicable sites in various seas worldwide could have served as case studies for this study. Due to the current global developments to simultaneously use marine areas and existing infrastructures according to the multi-use concept (Buck and Langan, 2017; Schupp et al., 2019) a region is chosen, where these concepts are being intensively investigated, such as the North Sea. North Sea countries including Germany, Denmark, the Netherlands, Belgium and the UK, have been studying the multi-use of offshore wind farms (OWF) and aquaculture for two decades and provide a wide range of data. We have focused on the German Bight due to the accessibility of suitable data. Synoptic data stemming from a numerical model covering the region and spanning a simulation period of two decades serves as basis for applying different exposure indices developed throughout this work to a continuous spatial data set (Hagen et al., 2021). The model data features a spatial resolution of 100 m and presents a range of hydrodynamic and morphologic variables. From the EasyGSH database, hydrodynamic quantities were obtained in georeferenced Tagged Image File Format (geoTIFF), which are subsequently processed with open

source and proprietary software (The Mathworks Inc, 2022; QGIS Development Team, 2022).

2.3.2 Extreme value analysis of hydrodynamic variables

Extreme value analysis of significant wave heights, $H_s(x,y)$, and depth averaged current speeds taken from the seabed to the free surface η, $\frac{1}{\eta+d}\int_{-d}^{\eta} U_c(x,y,z)dz$, from the EasyGSH database spanning 20 years (1996-2015) define estimates of the 50 year return values over a 100 m grid with dimensions 2141 x 2102 (n=2,789,571). The EasyGSH data repository provides bathymetry and yearly maxima significant wave heights on this 100 m grid and depth averaged currents (Δt=20 min), resampled to a 1000 m grid. Univariate extreme value analysis of significant wave heights and depth averaged current speeds was performed with series of yearly block maxima over the German Bight. This approach is conservative, as the directionality and behavior of extremes in the joint H_s-T_p-U distribution is not taken into account (e.g., 50-year u_w and U_c values are not necessarily coincident in time and direction). The authors acknowledge more robust methods exist for estimating extremes in a multivariate parameter space (Eckert-Gallup et al., 2016; Mackay and de Hauteclocque, 2023). At each node in the EasyGSH domain, series of yearly block maxima x_i, where x_i represents series of either hydrodynamic variable, were fit to the Gumbel distribution

$$F(x;\mu,\ \beta) = \exp(-e^{-(x-\mu)/\beta}),\quad -\infty < x < \infty \tag{21}$$

where μ is the location parameter and β>0 the scale parameter. The Gumbel distribution was selected after fitting at 500 random nodes to a range of distributions, and then assessing the quality of fits. The Gumbel distribution proved to fit best for 94% of the random sample.

The best fit to the Gumbel distribution was calculated through finding the least squares solution to

$$-\log(-\log(F(x;\mu,\ \beta))) = (x-\mu)/\beta. \tag{22}$$

The 50-year return values, x_{50}, were calculated from the associated fit, as:

$$x_{50} = \beta - \mu\log\left(-\log\left(1-\frac{1}{50}\right)\right). \tag{23}$$

Values of 50-year significant wave heights were assumed to have peak periods defined by wave steepness limits (DNVGL, 2010). Values of 50-year depth averaged currents were linearly interpolated to the same 100 m grid as 50-year significant wave heights and assumed to follow a power law over the depth. This resulted in current flow velocities (Equation 24) that can be used in calculation of exposure indices (Welzel et al., 2021; Lewis et al., 2017):

$$U(z) = U(0)\left(\frac{d+z}{d}\right)^{1/7},\quad z \le 0 \tag{24}$$

The 50-year H_s and associated T_p were used to calculate the maximum wave induced horizontal velocity magnitude $u_w(z)$, for z = 0 and -5 M.S.L. Lastly, bathymetry from EasyGSH was adjusted nearshore from its mean-sea-level datum to account for depth limited wave breaking that may have occurred during periods of high water (e.g., spring tide or storm surge). In locations where the 50-year H_s/d ratio was greater than 0.55, the depth was modified such that $d = H_s/0.55$.

2.3.3 Computation of exposure indices

The exposure indices from Section 2.1.2 were then computed for the grid cells of the synoptic numerical results of the 50-year extreme values. For the maps of the German Bight, constructed, commissioned and planned offshore wind park areas are also provided (Hannemann, 2022), since there has been a considerable body of literature that discusses multi-use concepts involving offshore wind and aquaculture production (Przedrzymirska et al., 2021; Gimpel et al., 2015; Buck et al., 2008; Buck and Langan, 2017). Vertical location in the water column considered for index calculations was set to the surface at z = 0 m except for the EVRD, which used z = -5m. For the structure-centric indices (SDE and SDBR) solidity was set to S = 0.25 and the characteristic length/diameter was set to D = 1.0 m, based on typical aquaculture structures.

Computed index values were normalized to render results more intercomparable. Methodological details are given appendix A.

3 Results

Hydrodynamic exposure indices developed in this study are applied to illustrate their applicability with respect to quantifying exposure of aquaculture sites or gear. To test universal applicability, a global perspective is given through mapped known global aquaculture sites where operational research or commercial farms are active. While these locations are single positions around the globe, hydrodynamic exposure indices can also be mapped for larger regions, as long as suitable basis input variables are available (see Section 2.1.1) The authors have used publicly available synoptic oceanographic data for the North Sea part of the German Bight to showcase the robustness and usefulness of the defined indices and examine their variations over a defined region.

3.1 Index comparison based on known aquaculture locations

We applied the six different Exposure Indices to quantify the exposure of known aquaculture locations. The resulting EI values are compiled in Table 1 with their respective location and corresponding return periods. The results have been color-coded with a color intensity proportional to index value magnitude; a mapped illustration is compiled in Figure 2 for the sites. Areas clustered with sites like northern Europe or the United States Atlantic and Pacific coast feature in Figures 3A–F respectively, to make the results more accessible on a regional scale. It is noted that index values in Table 1 are a function of return period and the values provided for this analysis are for a range of return periods including 10, 50, and 100 years.

It has to be noted that mapped locations are generally close to shore or port, and the advent of aquaculture production far offshore has not yet been seen. This corroborates Clawson et al. (2022) who state that 98% of the world's ocean space has no aquaculture operations.

From Figure 2, it is evident that the SDE is much more dependent on local differences in exposure than on global trends. Generally, most of the EI exhibit similarly high values for some of the highly exposed locations, such as sites 7, 8, 18 and 24. As desired, sheltered areas appear to exhibit lower index values, whereas unsheltered areas show higher values. Milder conditions according to the index are present inside the North Sea near the German Bight (cf. Figure 3A) as well as along the Atlantic coast of Ireland (cf. Figure 3B). The Faroe Islands (Figure 3C) show fairly mild conditions across all six indices for two locations described as sheltered (sites 24 and 25), whereas the northernmost site, open to the Arctic Sea (site 26) exhibits very exposed conditions according to the developed classification.

Conditions for the chosen aquaculture sites on the Pacific coast of the United States (i.e., site 6) are milder according to the Depth-integrated energy indices (DEF and SDE) but show more severe values for EV, EVRD, SEE and SDBR (c.f. Figure 3D). The Gulf of Mexico (site 8 in Figure 3E) shows more energetic conditions probably due to the frequent appearance and landfall of hurricanes within this region (Zuzak et al., 2021). For the Gulf of Maine along the Atlantic coast of the United States (cf. Figure 3F) the velocity-based exposure indices EV, EVRD, SEE and SDBR show larger values, whereas Depth-integrated energy and energy flux indices DEF and SDE represent sites 1, 4 and 5 as milder.

3.2 Influence of return periods

The sensitivity to return period was investigated based on available data for a location in New Zealand (see Table 2). The return periods assigned to the wave data are one and fifty years respectively. A longer return period would in general result in higher exposure indices. This reflects that the exposure indices are sufficiently flexible to quantify the intensity of conditions to which aquaculture gear will be exposed in shorter periods (e.g., a typical year) and longer periods (e.g., 50 years). For the various exposure indices, the ratio between the 50-year index value and the 1-year index value ranges from 1.6 to 3.5. Higher ratios were found for the indices that are approximately proportional to fluid drag loads (SEE and SDBR).

3.3 Spatial mapping products: The German Bight case

In addition to globally distributed aquaculture sites presented in Section 2.2, a synoptic assessment based upon extreme value analysis of numerical hindcast data covering the German Bight was performed to evaluate the performance of the developed indices on a spatial level. Figure 4 shows the 50-year hydrodynamic variables H_s, u_W, *and* U_c and the depth d that define the exposure indices that are presented in the following subsection 3.3.1 In all figures, the color bar scale spans from 0 to the 99th-percentile of the exposure index.

3.3.1 Exposure velocity

The EV and EVRD for surface currents and a reference depth of 5 m are depicted in Figures 5–8 respectively. Both the EV evaluated at the surface and EVRD approach upper percentiles near the barrier islands and at the mouths of estuaries, where shoaling waves increase u_w and the convergence of tidal inlets amplifies U_c. The EV index values at the surface more noticeably exceeds EVRD in regions further from the coast (e.g., >20 km) because horizontal velocities induced by shallow water waves do not decay with depth. In the normalized maps, i.e., Figure 6 and Figure 8, it is apparent, that values of EV are generally larger than EVRD in tidal basins and behind the back-barrier islands.

3.3.2 Specific exposure energy

The SEE at the surface is quantified for z = 0 m and results compiled in Figure 9 for computed and in Figure 10 for normalized SEE values. Spatial variations are more readily observed due to the quadratic contribution of u_W and U_c. The largest SEE values are found on the exposed side of barrier islands where, where horizontal wave-induced velocities are magnified by shallow water, and near constrictions where tidal and storm-driven currents are highest. Select deep water regions with high significant wave heights and large current speeds (Figure 4C) also yield large SEE values. The SEE is significantly reduced from 7-8 J/kg to 2-4 J/kg in the back bays and the shoals of the estuaries.

3.3.3 Depth-integrated energy flux

The DEF (Figures 11, 12) presents an alternative representation of exposure in the spatial domain. At a distance of 40 km from the coast, the DEF obtains values of 120 – 160 kW/m while in shallow regions along the barrier islands and in estuaries the DEF is consistently 2-20 kW/m. This spatial variation is primarily driven by the decrease in the $\frac{1}{2}\rho\bar{U}_c^3 d$ term as d approaches 0 m in shallow waters and secondarily by the reduced 50-year sea states in protected waters.

3.3.4 Structure-centered depth-integrated energy

The SDE, evaluated with structure solidity of 0.25 and surface area $\pi/4$ in Equation 18, accentuates the energy in the deeper regions of estuarine channels and tidal inlets in the southern and south-eastern regions of the German Bight (Figures 13, 14). When water depths approach 0 m, the SDE is limited to values <50 kJ kg/m^3. In open water, the SDE obtains values of 1.5 to 23 kJ kg/m^3.

3.3.5 Structure-centered drag-to-buoyancy ratio

The SDBR at the surface is presented in Figures 15, 16, for SDBR values and its normalized version respectively. It is proportional to the SEE; it is greatest in nearshore waters exposed to 50-year sea states and amplified oceanic currents. In the leeward side of barrier islands, the SDBR is consistently less than 0.8 while it remains amplified in the center of estuarine channels.

TABLE 1 Oceanographic data for selected aquaculture sites around the globe. The colormap identifies the relative value of the EI with respect to the selected sites. Source is personal communication with.

ID	Location	Source	Return Period	Water Depth	Sig. Wave Height	Peak Period	Oceanic Current Speed	Position in Water Column	EV	EV 5m	SEE	DEF	SDE	SDBR
			yr	m	m	s	m/s	m	m/s	m/s	J/kg	kW/m	kJ kg/m^3	–
1	Gulf of Maine, Cape Elizabeth	Dewhurst	50.0	26.0	9.6	11.4	0.5	0.0	3.90	3.44	7.63	465.56	28.08	0.78
2	Gulf of Maine, Saco Bay	Dewhurst	50.0	14.0	5.4	11.4	0.8	0.0	3.19	2.93	5.24	150.45	9.72	0.42
3	Gulf of Maine, Cape Elizabeth (submerged)	Dewhurst	50.0	26.0	9.6	11.4	0.5	-3.0	3.61	3.44	6.53	465.56	28.08	0.52
4	Gulf ofMaine, Saco Bay (submerged)	Dewhurst	50.0	14.0	5.4	11.4	0.8	-3.0	2.99	2.93	4.61	150.45	9.72	0.37
5	Gulf of Maine, Isle of Shoals	Dewhurst	50.0	52.0	10.1	12.6	0.7	0.0	3.48	3.17	6.13	576.67	33.29	0.49
6	Santa Barbara Channel	Dewhurst	50.0	33.0	5.6	7.1	0.8	0.0	3.32	2.48	5.45	106.97	11.84	0.44
7	Gulf of Mexico, Pensacola	Dewhurst	50.0	45.0	12.2	15.0	2.0	0.0	5.33	5.02	14.00	1170.29	65.82	1.12
8	Gulf of Mexico, Pensacola (submerged)	Dewhurst	50.0	45.0	12.2	15.0	2.0	-15.0	4.63	5.02	10.53	1170.29	65.82	0.84
9	North Sea, FINO1	Strothotte	50.0	30.0	7.4	14.0	1.5	0.0	3.86	3.64	7.45	390.40	24.37	0.60
9a	North Sea, FINO1	*EasyGSH*	*50.0*	*29.96*	*5.84*	*7.31*	*1.46*	*0.0*	*4.02*	*3.27*	*8.07*	*142.63*	*17.78*	*1.65*
10	North Sea, Roter Sand	Buck	1.0	12.0	3.0	10.0	1.0	0.0	2.48	2.25	3.06	45.89	4.11	0.25
10a	North Sea, Roter Sand	*EasyGSH*	*50.0*	*10.8*	*4.39*	*7.0*	*1.62*	*0.0*	*4.08*	*3.29*	*8.31*	*75.86*	*9.15*	*1.69*
11	Opotiki, Bay of Plenty, New Zealand (submerged)	Heasman	50.0	45.0	7.6	15.2	0.6	-5.0	2.48	2.48	3.07	392.64	19.06	0.25
12	Pegasus Bay, New Zealand (submerged)	Heasman	50.0	22.0	7.6	15.2	0.6	-3.0	3.13	3.11	5.06	390.09	18.06	0.40
13	Boknafjorden, Norway	Moe Føre	50.0	100.0	2.5	6.0	1.0	0.0	2.31	1.75	2.67	67.81	13.93	0.21
14	Frohavet, Norway	Moe Føre	50.0	100.0	7.0	7.0	1.2	0.0	4.34	3.28	9.42	240.01	31.90	0.75
15	Long Island, Ireland		10.0	15.0	5.4	19.6	0.9	0.0	3.10	3.05	4.94	257.96	10.10	0.40
16	Cape Clear, Ireland		10.0	35.0	11.0	19.6	0.8	0.0	3.88	3.75	7.61	1056.35	38.54	0.61
17	Bantry Bay, Ireland		10.0	20.0	2.5	19.2	0.4	0.0	1.34	1.27	0.86	53.64	2.24	0.07
18	Deenish Island, Kenmare Bay, Ireland		10.0	27.0	12.7	19.3	0.5	0.0	4.51	4.33	10.23	1376.21	48.58	0.82

(Continued)

10.3389/faquc.2024.1388280

TABLE 1 Continued

ID	Location	Source	Return Period	Water Depth	Sig. Wave Height	Peak Period	Oceanic Current Speed	Position in Water Column	EV	EV 5m	SEE	DEF	SDE	SDBR
			yr	m	m	s	m/s	m	m/s	m/s	J/kg	kW/m	kJ kg/m^3	–
19	Clare Island, Clew Bay, Ireland		10.0	21.0	3.2	19.5	0.8	0.0	1.93	1.88	1.87	93.68	4.66	0.15
20	Clew Bay, Ireland		10.0	20.0	1.9	19.1	0.6	0.0	1.30	1.26	0.83	32.66	1.94	0.07
21	Caribbean Sea, Panama	Sclodnick & Sullivan	10.0	62.0	6.0	10.0	1.6	-15.0	2.65	3.16	3.52	289.11	29.83	0.28
22	Gulf of California, Baja California Sur, Mexico	Sclodnick & Sullivan	10.0	42.0	5.0	7.0	0.6	0.0	2.85	2.09	4.06	81.92	9.23	0.32
23	Fiskaaling 1, Faroe Islands	Norði via Strand via Dewhurst	50.0	20.0	4.5	16.0	0.2	0.0	1.86	1.75	1.74	143.14	6.09	0.14
24	Fiskaaling 2, Faroe Islands		10.0	33.0	14.0	16.0	0.3	0.0	4.51	4.18	10.03	1385.14	58.40	0.80
25	Gøtuvík, Faroe Islands	Joensen via Buck	50.0	70.0	7.0	10.0	0.7	0.0	2.95	2.55	4.36	230.89	19.14	0.35
26	Luderitz, Namibia	Knoester via Dewhurst	50.0	55.0	5.3	14.5	0.7	0.0	2.08	1.94	2.11	189.51	11.57	0.17
27	Thornton Bank, North Sea, Surfaced	Nevejan and Pribadi via Dewhurst	50.0	29.0	6.3	8.3	1.1	0.0	3.55	2.99	6.56	165.24	15.99	0.52
28	Thornton Bank, North Sea, Submerged		50.0	29.0	6.3	8.3	1.1	-9.0	2.57	2.99	3.45	165.24	15.99	0.28
29	Norwegian Sea, Frohavet	(Jin et al., 2021)	100.0	150.0	5.0	11.0	0.8	0.0	2.18	2.01	2.48	160.78	19.00	0.20

1) Ocean current speed (U_c) at z=0m was used as design current speed for the developed indices due to a lack of information regarding depth resolved ocean current profiles. For site specific applications the user is strongly advised to use depth resolving information for design related questions.
2) Lines 9a and 10a are derived from statistical extrapolation of 20 year numerical simulation to 50 year return period values extracted from the areal representations given in Figures 5–16.
3) Color intensity for last six columns is based on cell value, with faded to most intense correlating to smallest to largest value.

10.3389/faquc.2024.1388280

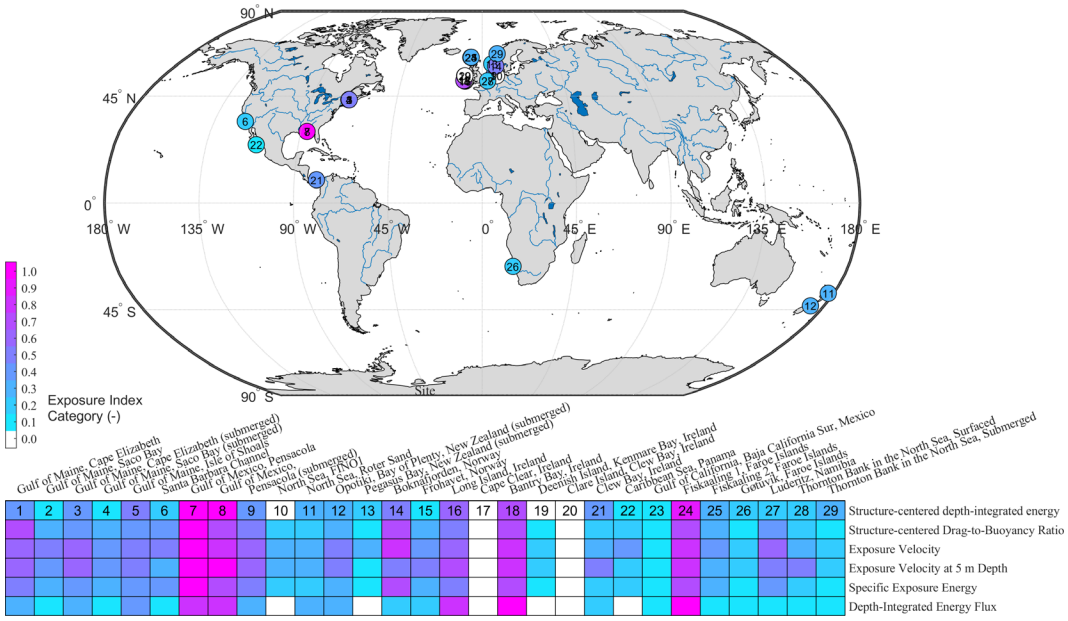

FIGURE 2
Mapping of selected aquaculture structure locations, associated with the six suggested exposure index definitions as per sub-section Hydrodynamic exposure indices Tabulated exposure indices, color-coded by normalized index values per index based on data compiled in Table 1. Map icons are color-coded according to the top-row of the index table (Table 1) representing the Structure-centered depth-integrated energy (SDE).

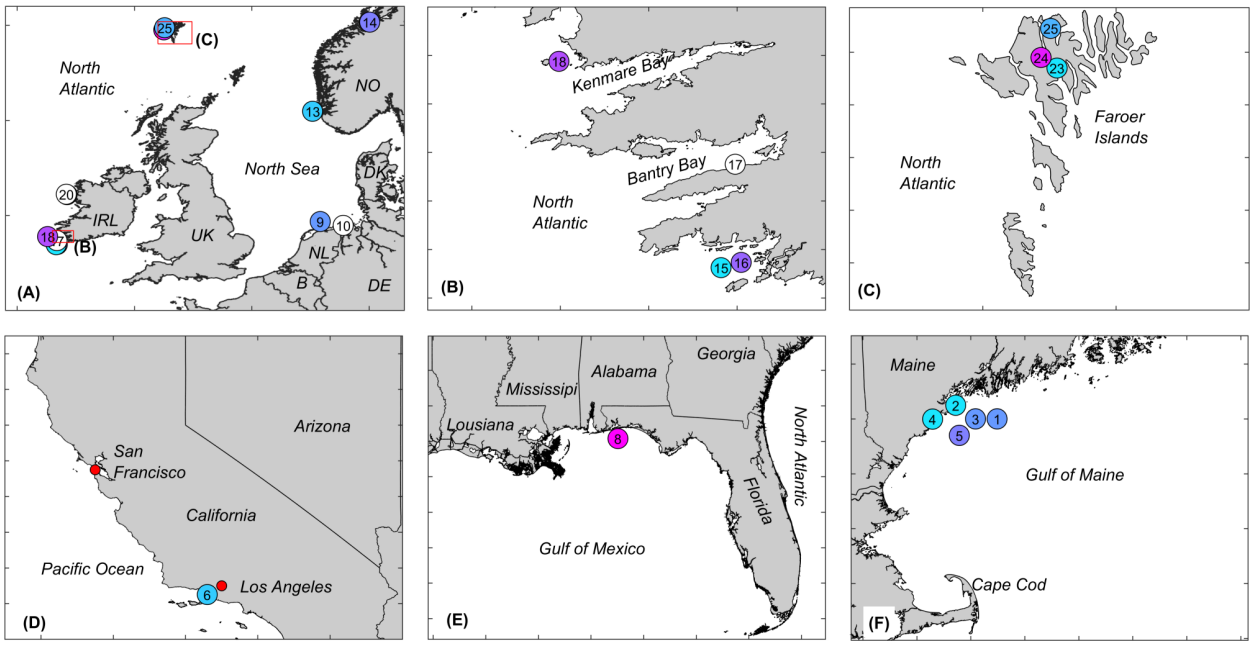

FIGURE 3
Select magnifications of exposure sites with **(A–C)** in northern Europe and **(D–F)** in North America. Color coded exposure index sites are based of the Structure-centered depth-integrated energy (SDE) index from the top row of the bottom panel in Figure 2 The SDE is mapped for **(A)** Northern Europe, with **(B)** Ireland harbouring multiple sites and three more situated on **(C)** the Faroe Islands. For the Pacific **(D)** a site is characterized near LA, with a site at the coast of the Gulf of Mexico **(E)** and multiple sites located within the Gulf of Maine **(F)**.

TABLE 2 Comparison of impacts of return periods (1versus 50 years) on the different exposure indices for a given location.

ID	Location	Source	Return Period	Water Depth	Sig. Wave Height	Peak Period	Oceanic Current Speed	Position in Water Column	EV	EV at 5 m depth	SEE	DEF	SDE	SDBR
			yr	m	m	s	m/s	m	m/s	m/s	J/kg	kW/m	kJ kg/m^3	–
11	Opotiki, Bay of Plenty, New Zealand (submerged)	0 Heasman	1	45	4.6	12.0	0.3	-5.0	1.5	1.5	1.2	125.5	7.5	0.16
11	Opotiki, Bay of Plenty, New Zealand (submerged)	0 Heasman	50.0	45.0	7.6	15.2	0.6	-5.0	2.48	2.48	3.07	392.64	19.06	0.25
Ratio of 50-year value to 1-year value					1.7		2.0		1.6	1.6	2.6	3.5	2.8	2.6

1) Colors matching to previously used scheme in Table 1 for ease of comparison.

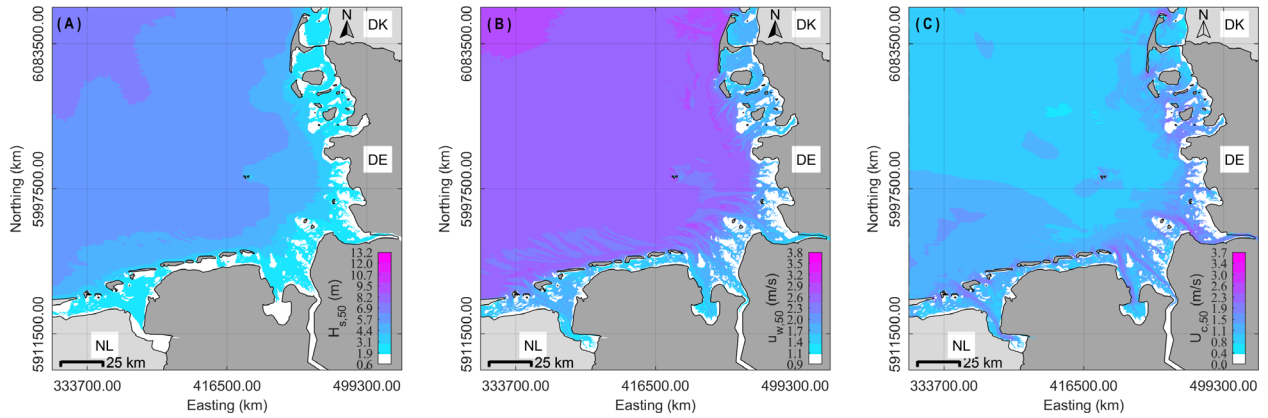

FIGURE 4
From left to right, the 50-year **(A)** H_s, **(B)** u_w at the surface, and **(C)** depth averaged U_c. Bathymetry (black contour) is shown for z = 20 m and z = 40 m, while the upper limit of the color bar in **(B)** and **(C)** is the 99th-percentile of u_w. These values are estimated from hindcast data and should not be used for design.

4 Discussion

4.1 Relation to other previously proposed indices

The study at hand concentrates on environmental conditions and structure-related characteristics to assess the exposure of various sites. In comparison, Calleja et al. (2022) included species related prerequisites for a successful cultivation covering waves and currents as well but also including sea surface temperature, salinity and optical water clarity in coastal waters. Furthermore, they matched potential sites with other coastal stakeholders and activities such as energy production, shipping or recreation and assessed potential for upkeep such as maintenance, feeding and accessibility. A similar approach was presented by Benetti et al. (2010) in a broad study on site selection procedure for open ocean aquaculture. Similar to Calleja et al. (2022), that proposed classification scheme omitted the need to assess ocean site specific exposure and concentrated on species related aspects. However, neglecting to assess environmentally based physical conditions such as ocean currents, wave climate and water depths and structure related properties and performance can easily end in uneconomic scenarios. In contrast, no biological characteristics have been included in the development of the indices presented in this work. Species connected cultivation optima have been considered to be secondary in this study and subject to a different work in the special issue (Heasman et al., 2024). These exposure indices primarily relate the to the cultivation structures that must be planned, constructed and maintained in challenging conditions. However, it is quite possible that the suitability of various aquaculture species for certain sites may be similarly quantified using the proposed exposure indices.

The indices presented are based on physical abiotic parameters alone. Consequently, they do not cover water temperature, nutrients, or turbidity. Such parameters are of interest to aquafarming in that they confine the range of species which can potentially be cultivated at a given site. Nevertheless, this can be overcome by adding additional index metrics for those aspects of mariculture and does not preclude the identification of beneficial cultivation sites. Another parameter not covered by the indices

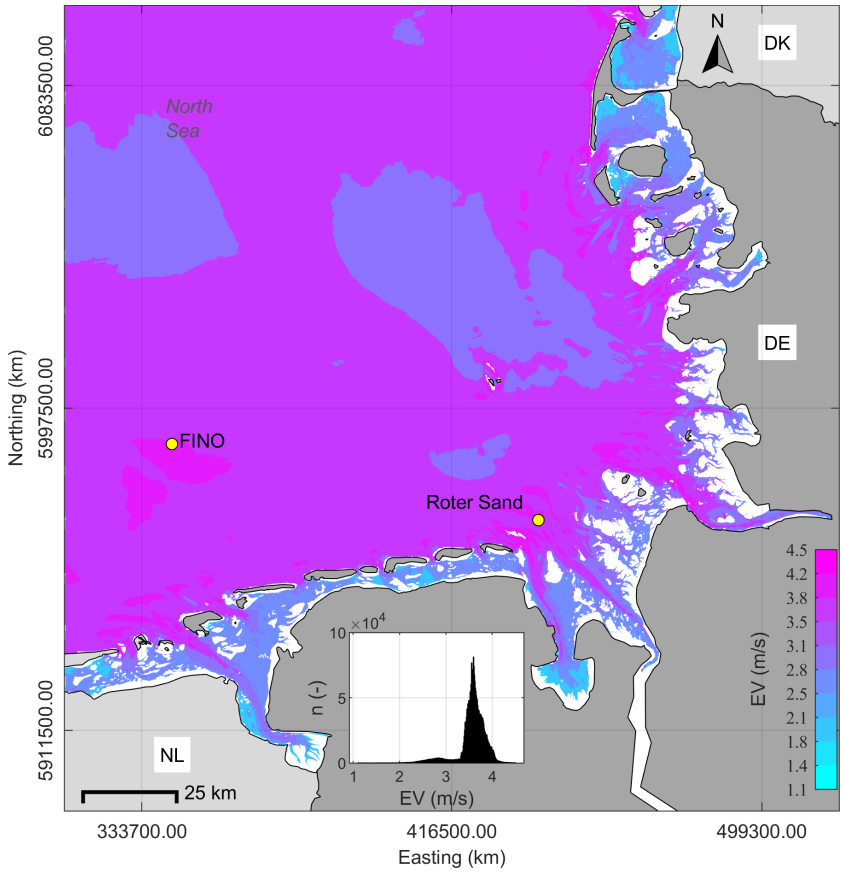

FIGURE 5
Exposure Velocity (EV) for 50-year surface currents.

presented constitutes wind speed, which might be an important aspect for certain types of open ocean structures depending on their profile above the water line. In addition, wind speed, like waves and currents, will certainly affect harvesting operations and could therefore be also included in a broader framework for mariculture site assessment in future works.

Future developments of further indices or the refinement of other approaches can therefore easily be integrated into the classification approach presented in Section 2.1 This will allow for future aquaculture sites to be easily assessed with multiple perspectives in mind. For example, an integration or addition of species-specific ocean condition requirements could be added. Another extension could entail an investment perspective, depending on the structure in question e.g., floating or anchored, near or far from land, and further enhance the classification.

4.2 Observations from mapping indices on the global and regional scales

Among 29 sites, high energy conditions resulted in high index values for sites fully exposed to the North Atlantic (cf. Figure 2E sites 16 & 22), the Gulf of Mexico (cf. Figure 2E sites 7 & 8), and the Arctic Ocean (cf. Figure 2C site 27) for the data provided for a return period of 50 years. In the Gulf of Mexico, the annual occurrence of Hurricanes within this region is expected to constitute a major driver for these values (Zuzak et al., 2021). Similarly, the Atlantic coast of Ireland is frequently impacted by extratropical cyclones following an eastward trajectory across the North Atlantic in the winter season (European Commission. Joint Research Centre, 2020). All other sites fall below these hotspots regarding exposure index values.

Figure 5 through Figure 16 show that certain *sites can simultaneously be close to land and highly exposed*. With the exception of the depth-integrated indices, the proposed indices show that in the German Bight, the regional focus we chose for this work, high exposure values are found on the seaward sides of the barrier islands, where large waves enter shallow water, producing very large oscillating fluid particle velocities and resulting drag forces, and near constrictions that amplify current velocities. In contrast, many of the indices show a markedly sheltered region East of the island Heligoland which is less exposed by larger waves.

4.3 Comparison of proposed indices

The EV and EVRD have the beneficial quality of being straightforward and easily comprehensible, with well-understood units (velocity). They, along with the SEE and SDBR, capture the large fluid velocities that can occur even in shallow, nearshore sites.

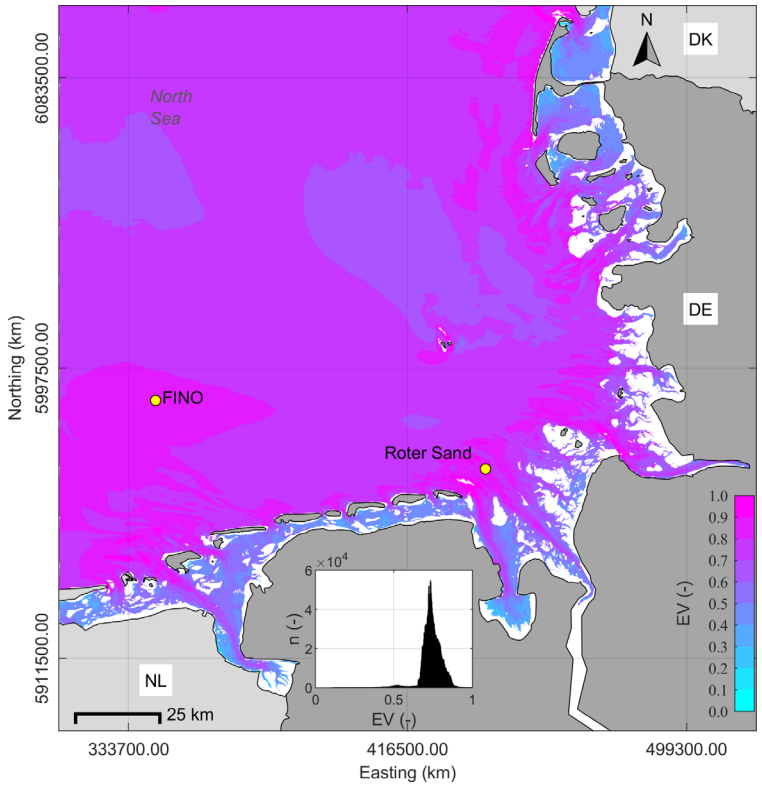

FIGURE 6
Normalized Exposure Velocity (EV) for 50-year surface currents.

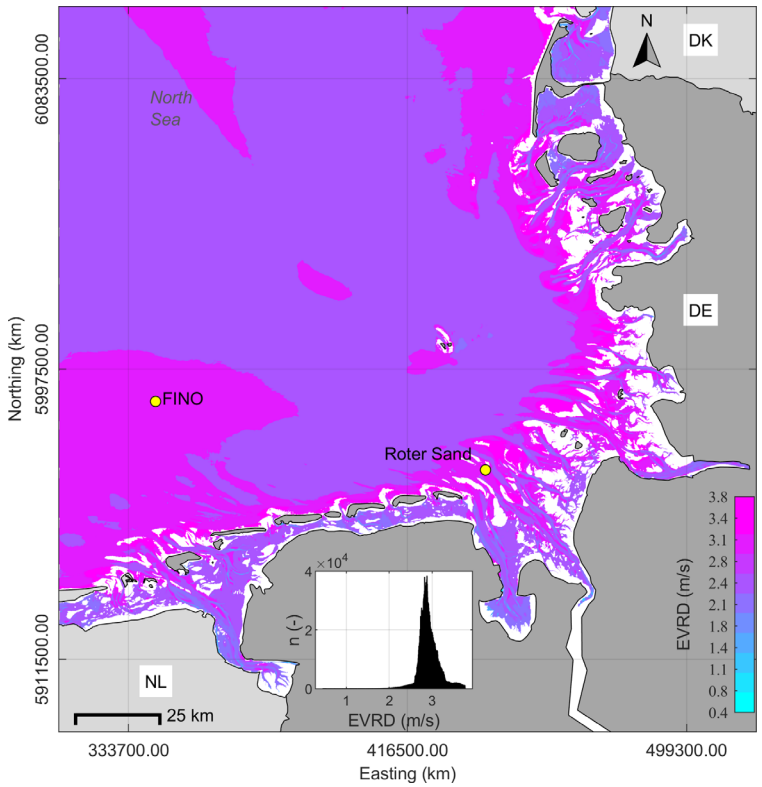

FIGURE 7
Exposure Velocity at Reference Depth (EVRD) at 5 m below the surface for 50-year surface currents.

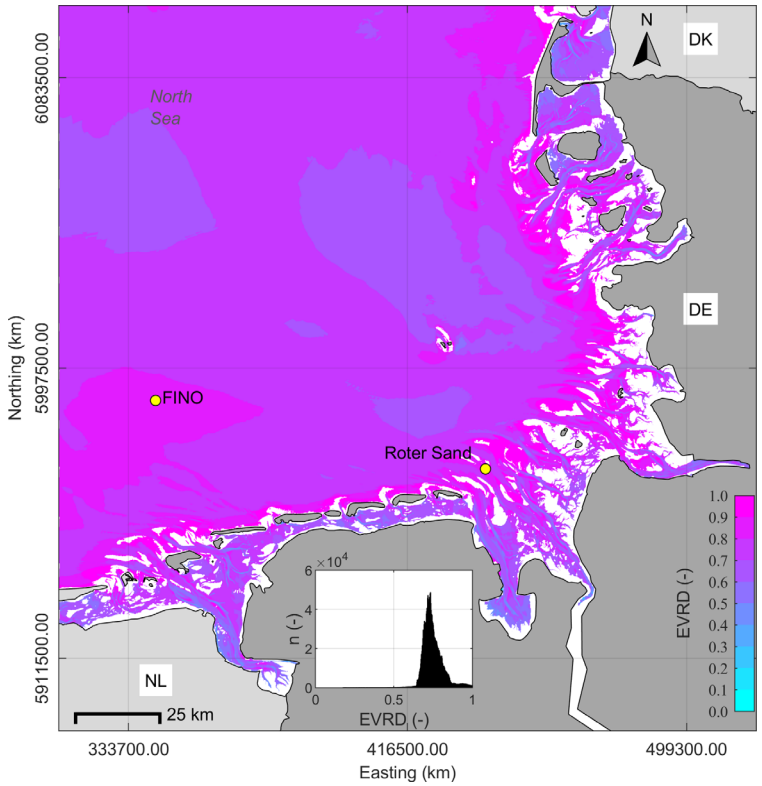

FIGURE 8
Normalized Exposure Velocity at Reference Depth (EVRD) at 5 m below the surface for 50-year surface currents.

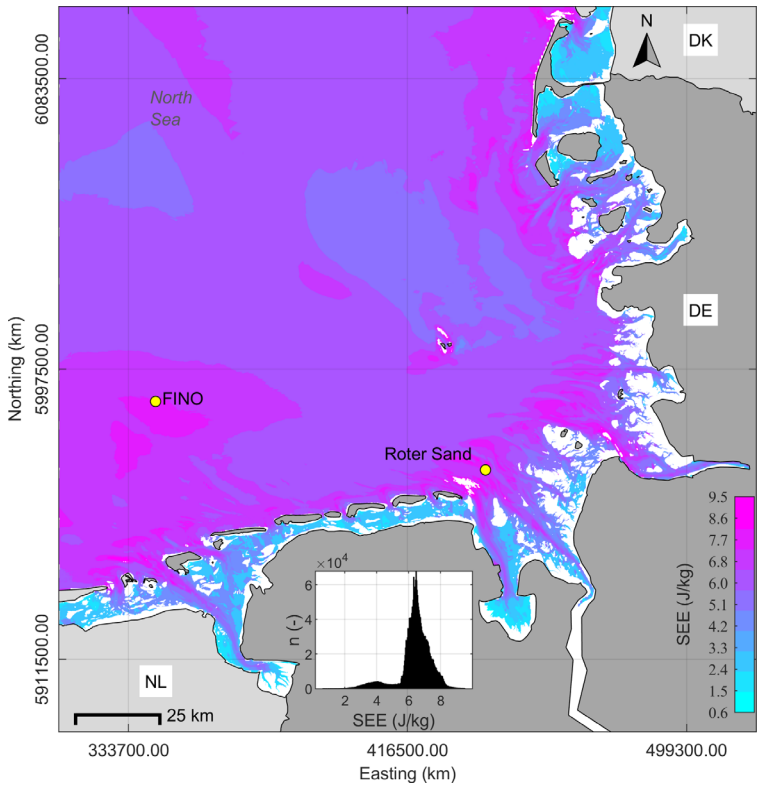

FIGURE 9
Specific Exposure Energy (SEE) for 50-year surface currents and wave induced velocities.

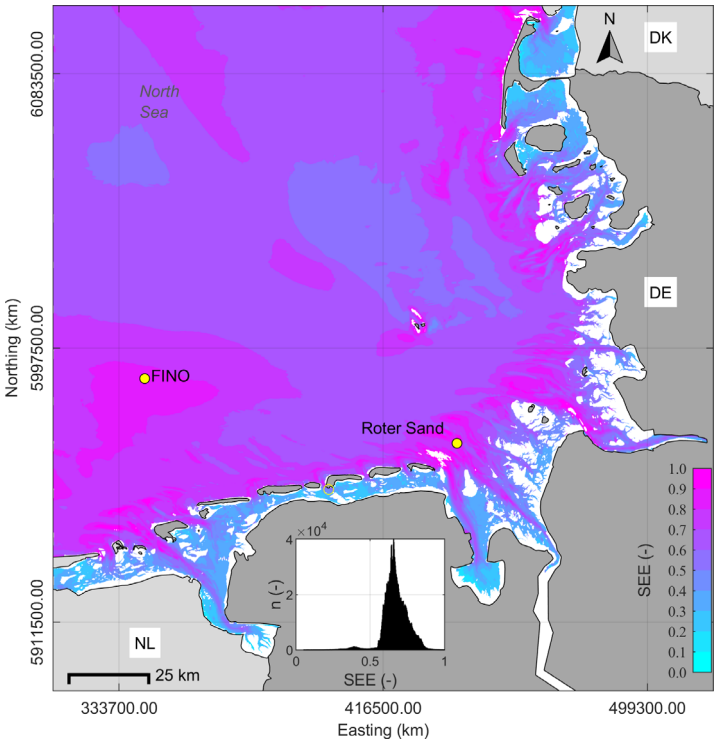

FIGURE 10
Normalized Specific Exposure Energy (SEE) for 50-year surface currents and wave induced velocities.

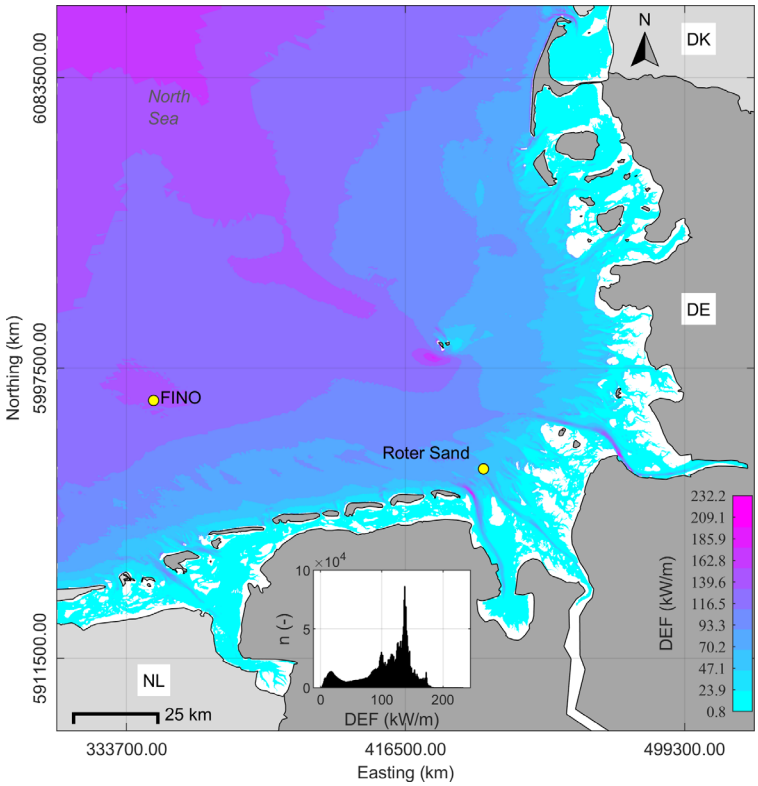

FIGURE 11
Depth-integrated Energy Flux (DEF) evaluated with 50-year depth averaged currents and with the deep water wave energy flux for 50-year sea states.

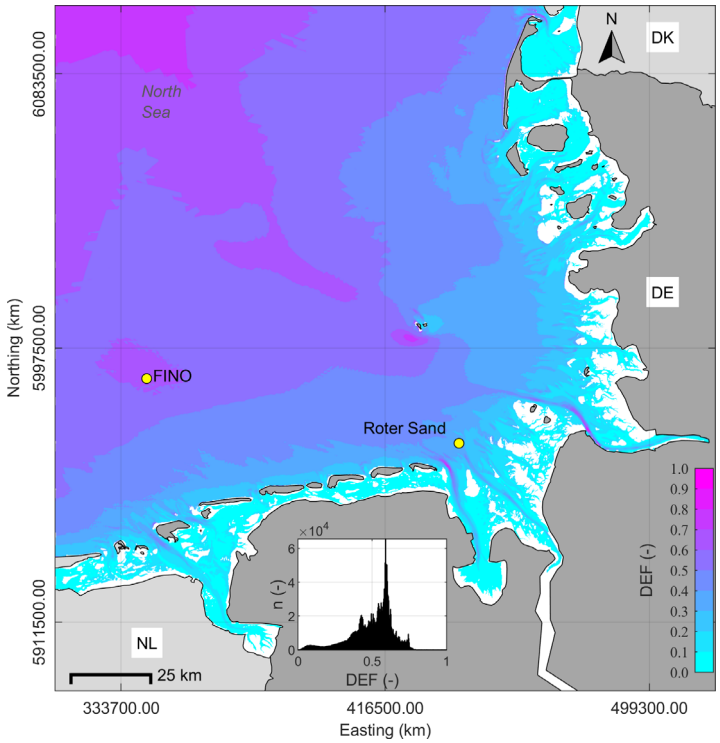

FIGURE 12
Normalized depth-integrated Energy Flux (DEF) evaluated with 50-year depth averaged currents and with the deep water wave energy flux for 50-year sea states.

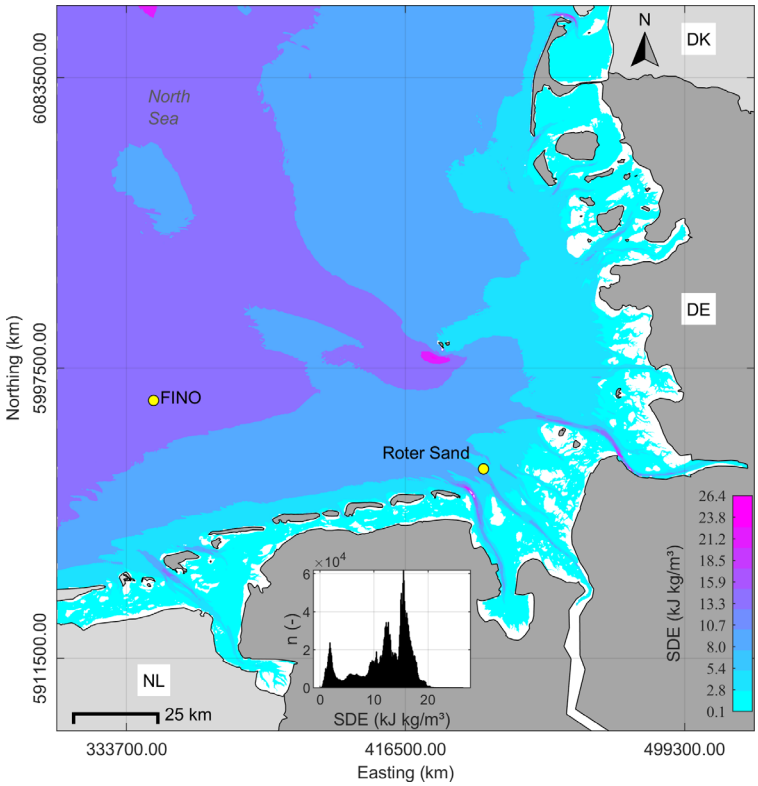

FIGURE 13
Structure-centered Depth-integrated Energy (SDE) associated with the 50-year significant wave heights and depth averaged currents, with constant density 1025 kg/m3, structure solidity of 0.3 and surface area $\pi/4$.

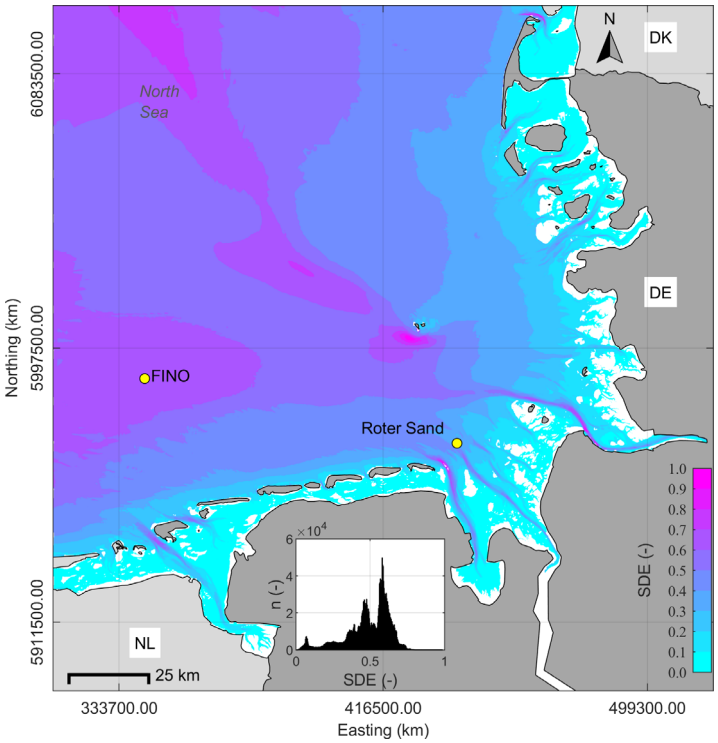

FIGURE 14
Normalized Structure-centered Depth-integrated Energy (SDE) associated with the 50-year significant wave heights and depth averaged currents, with constant density 1025 kg/m3, structure solidity of 0.3 and surface area $\pi/4$.

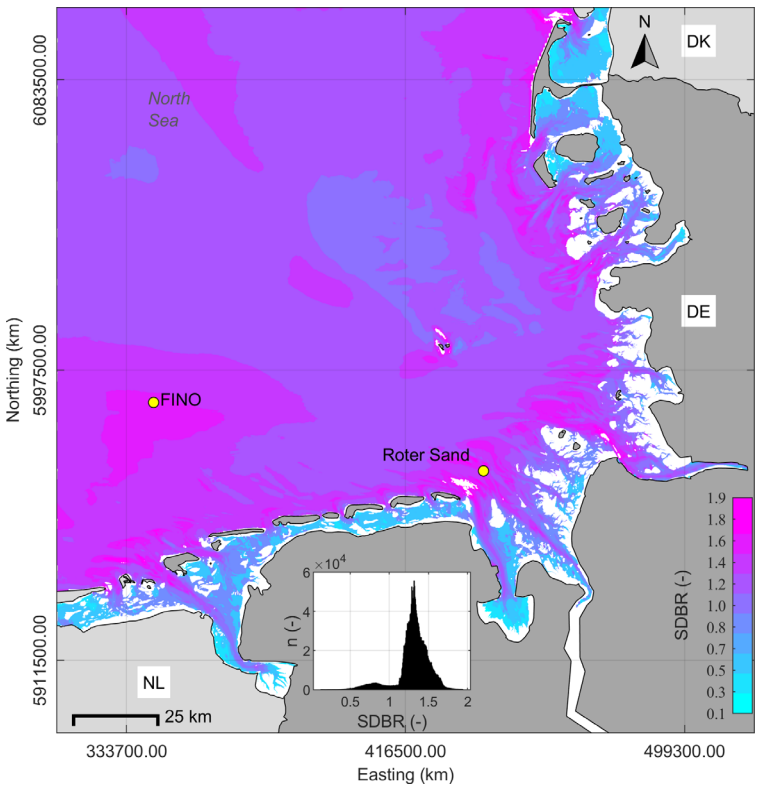

FIGURE 15
Structure-centered Drag-to-Buoyancy Ratio (SDBR) evaluated with 50-year surface u_w and Uc and D = 1 m is non-dimensional and proportional to the SEE.

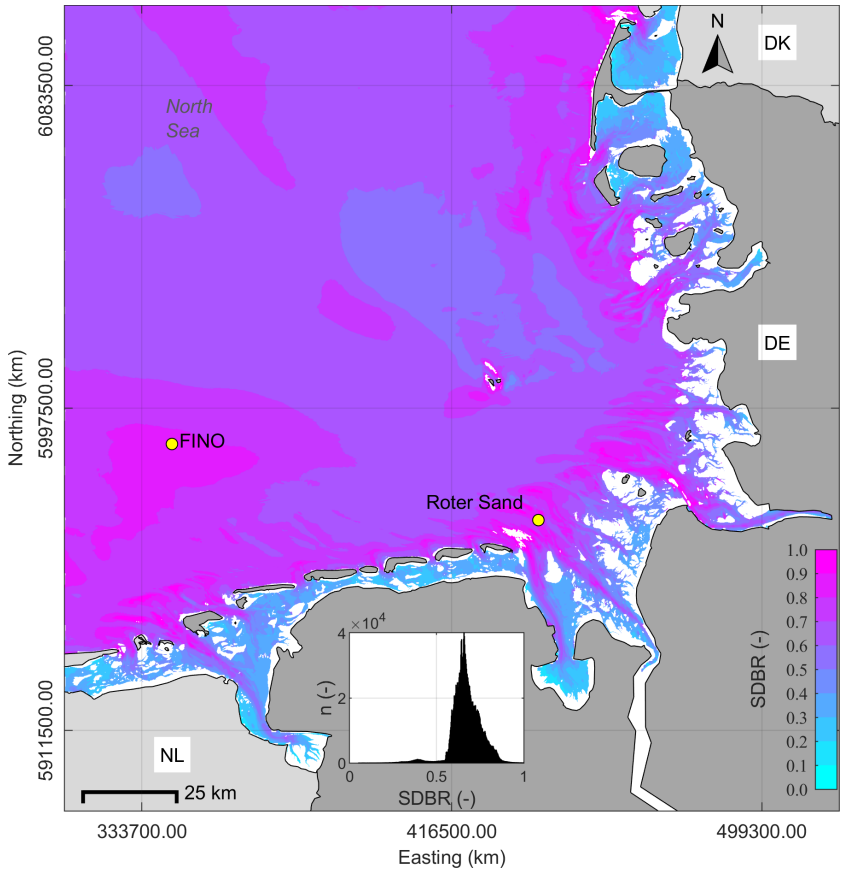

FIGURE 16
Structure-centered Drag-to-Buoyancy Ratio (SDBR) evaluated with 50-year surface uw and Uc and D = 1 m is non-dimensional and proportional to the SEE.

The SEE has the additional qualities of being proportional to both kinetic energy and fluid drag, while it has physically meaningful units (kinetic energy per mass of water, J/kg in SI). Figure 9 shows that this index (as with the SDBR) provides a large range of differentiation between index values for sheltered and exposed sites even in close proximity (e.g., on either side of a barrier island).

The depth-integrated, energy-based indices (DEF and SDE) are convenient in that they do not require the calculation of wave kinematics described in Section 2.1.1 and show that these indices increase significantly with deep water generally found far from shore, these values may not be closely tied to the magnitude of forces on floating structures.

Like the SEE, the SDBR has qualities of being proportional to both kinetic energy and fluid drag. It has the additional quality of being non-dimensional. Since this is accomplished by incorporating a characteristic length for the structure, this index depends on knowledge or assumptions about the selected gear type.

The six indices appear to provide quick and plausible site characterizations. However, no single index has been determined to outperform the others. They appear to be complementary, each with strengths and weaknesses. The authors herein present the indices to the aquaculture and ocean engineering communities for discussion, application, potential adoption of one or more of the proposed indices. Table 3 summarizes key aspects of the EI formulations, using criteria such as the applicability with respect to the dimensionless water depth, the complexity (for layperson), strength and weaknesses of the EI formulation.

This work has, through intense discussions within the author collective, decided to select two of the six indices to continue to work with; the selection has been made based on some of the arguments pondered on in the discussion section, summarized in Table 3. Heasman et al. (2024) will continue to work with the two selected indices EVRD and SEE.

5 Conclusion

Bearing in mind the basic goals laid out at the end of Section 1, a broad and objective formulation of hydrodynamic exposure has been accomplished and exposure indices been introduced. Through the application of the exposure indices to known aquaculture sites around the globe, their respective performance has been assessed across six indices. The sensitivity towards return periods of ocean conditions has been investigated and discussed in Section 3.2 Furthermore, the indices have been applied on a basin wide synoptic scale, showcasing their performance for the rough North Sea (cf. Section 3.3). The advantages and caveats of the indices introduced were laid out and discussed. In addition, the developed approach has been compared to other indices found in literature (cf.

TABLE 3 Overview over specific aspects of the six presented EI, using common criteria.

	EV	EVRD	SEE	DEF	SDE	SDBR
Applicability for d/L	all water depth	all water depth	all water depth	> 0.5, only deep water	all water depth	all water depth
Complexity	low	low	low	high	low	low
Strength of index formulation	easy application	easy application	Strength in physics-based formulation	Inclusion of potential energy	formulation gives units of energy	Normalization straight-forward
Selected limitations of index formulation	Dominant focus on velocity alone	See EV	-/-	-/-	considers entire water depth, while gear could be only close to surface	Composed of Dimensionless numbers, potentially difficult to grasp

Section 4). Rigorous calculation and mapping of 50-year extreme storm conditions for the German Bight, with results entered as inputs to the exposure indices, showed that sites can simultaneously be close to shore and highly exposed. This demonstrates the need to separate the term "offshore" into two separate metrics: exposure and distance from land. With the proposed indices, it is now possible to objectively quantify exposure on a continuum according to the severity of ocean conditions. The approach presented by this study is limited only by the availability of data for a respective site. Thus, the indices presented are globally applicable for characterizing potential mariculture sites. The novelty of this study compared to other classification studies for mariculture sites pertains to the assessment of physical ocean exposure characteristics, which are generally omitted by other assessment metrics. This may result in non-economic designs. The six EI proposed in this study solely focus on abiotic aspects for characterizing mariculture sites. However, species related biotic factors, such as water temperature can be easily added and are the focus future work. Another important aspect that has not been included in the EI proposed here constitutes wind speed, which drives wave mechanics and is also a focus for future work. Furthermore, the EI presented here clearly show, that unsheltered sites closer to major storm pathways like the Gulf of Mexico, the North Atlantic or Arctic Ocean exhibit higher values. Simultaneously, shallower and more sheltered areas behind barrier islands or within bays exhibit more favorable oceanic exposure conditions.

Data availability statement

The data analyzed in this study is subject to the following licenses/restrictions: Non-public data will be made available upon reasonable request. Requests to access these datasets should be directed to Nils Goseberg, n.goseberg@tu-braunschweig.de.

Author contributions

OL: Data curation, Formal analysis, Software, Supervision, Visualization, Writing – original draft, Writing – review & editing. NG: Conceptualization, Investigation, Methodology, Supervision, Validation, Visualization, Writing – original draft, Writing – review & editing. HF: Conceptualization, Data curation, Methodology, Writing – review & editing. TD: Conceptualization, Data curation, Formal analysis, Methodology, Validation, Writing – review & editing. TB: Data curation, Software, Visualization, Writing – review & editing. KH: Conceptualization, Methodology, Validation, Writing – review & editing. BB: Conceptualization, Methodology, Writing – review & editing. DF: Conceptualization, Methodology, Visualization, Writing – original draft, Writing – review & editing. SR: Data curation, Formal analysis, Software, Visualization, Writing – review & editing.

Funding

The author(s) declare financial support was received for the research, authorship, and/or publication of this article. Contributions have been supported by the SFI EXPOSED research center, financed by the partners and the Research Council of Norway under grant number 237790. We acknowledge support by the Open Access Publication Funds of Technische Universität Braunschweig.

Acknowledgments

The author collective is indebted to the following individuals for providing constructive input in the form of data, site knowledge or subjective wisdom about perceived experience to hydro-environmental conditions in real mariculture sites: Michael Chambers, John Holmyard, Frank Kane. This publication was prepared within the scope of the WGOOA (Working Group on Open Ocean Aquaculture) of the intergovernmental science organization ICES (International Council for the Exploration of the Sea - Copenhagen/Denmark). This work has been published with the financial support by the Open Access Publication Funds of the Technische Universität Braunschweig.

Conflict of interest

Authors TD and SR were employed by the company Kelson Marine Co.

The remaining authors declare that the research was conducted in the absence of any commercial or financial relationships that could be construed as a potential conflict of interest.

Publisher's note

All claims expressed in this article are solely those of the authors and do not necessarily represent those of their affiliated organizations, or those of the publisher, the editors and the reviewers. Any product that may be evaluated in this article, or claim that may be made by its manufacturer, is not guaranteed or endorsed by the publisher.

Supplementary material

The Supplementary Material for this article can be found online at: https://www.frontiersin.org/articles/10.3389/faquc.2024.1388280/full#supplementary-material

References

Aguilar-Manjarrez, J., Soto, D., and Brummett, R. E. (2017). "Aquaculture zoning, site selection and area management under the ecosystem approach to aquaculture," in *A handbook / josé Aguilar-manjarrez, doris soto and randall brummett* (Food and Agriculture Organization of the United Nations/The World Bank, Rome).

Ahn, S. (2021). Modeling mean relation between peak period and energy period of ocean surface wave systems. *In Ocean Eng.* 228, 108937. doi: 10.1016/j.oceaneng.2021.108937

Benetti, D. D., Benetti, G. I., Rivera, J. A., Sardenberg, B., and O'Hanlon, B. (2010). Site selection criteria for open ocean aquaculture. *In Mar. Technol. Soc. J.* 44, 22–35. doi: 10.4031/MTSJ.44.3.11

Boyd, C. E., D'Abramo, L. R., Glencross, B. D., Huyben, D. C., Juarez, L. M., Lockwood, G. S., et al. (2020). Achieving sustainable aquaculture: Historical and current perspectives and future needs and challenges. *In J. World Aquacult Soc.* 51, 578–633. doi: 10.1111/jwas.12714

Buck, B. H., Bjelland, H. V., Bockus, A., Chambers, M., Costa-Pierce, B. A., Dewhurst, T., et al. (2024). Resolving the term "offshore aquaculture" by decoupling "exposed" and "distance from the coast. *Front. Aquac.* 3, 1428056. doi: 10.3389/faquc.2024.1428056

Buck, B. H., and Grote, B. (2018). "Seaweed in high-energy environments. Protocol to move Saccharina cultivation offshore," in *Protocols for macroalgae research, vol. 1.* Eds. B Charrier, T. Wichard and C. R. K. Ry (CRC PRess, Boca Raton). doi: 10.1201/b21460-1/seaweed-high-energy-environments-bela-buck-britta-grote

Buck, B. H., Krause, G., Michler-Cieluch, T., Brenner, M., Buchholz, C. M., Busch, J. A., et al. (2008). Meeting the quest for spatial efficiency: progress and prospects of extensive aquaculture within offshore wind farms. *In Helgol Mar. Res.* 62, 269–281. doi: 10.1007/s10152-008-0115-x

Buck, B. H., Krause, G., and Rosenthal, H. (2004). Extensive open ocean aquaculture development within wind farms in Germany: the prospect of offshore co-management and legal constraints. *In Ocean Coast. Manage.* 47, 95–122. doi: 10.1016/j.ocecoaman.2004.04.002

Buck, B. H., and Langan, R. (Eds.) (2017). *Aquaculture perspective of multi-use sites in the open ocean* (Cham: Springer International Publishing).

Calleja, F., Chacón Guzmán, J., and Alfaro Chavarría, H. (2022). Marine aquaculture in the pacific coast of Costa Rica: Identifying the optimum areas for a sustainable development. *In Ocean Coast. Manage.* 219, 106033. doi: 10.1016/j.ocecoaman.2022.106033

Chao, F., Gerland, P., Cook, A. R., and Alkema, L. (2021). Global estimation and scenario-based projections of sex ratio at birth and missing female births using a Bayesian hierarchical time series mixture model. In. *Ann. Appl. Stat.* 15, 1499-1528. doi: 10.1214/20-AOAS1436

Chopin, T., and Sawhney, M. (2009). "Seaweeds and their mariculture," in *Encyclopedia of ocean sciences* (Marine Policy Center, Woods Hole Oceanographic Institution, Woods Hole, Massachusetts, USA: Elsevier), 317–326.

Clawson, G., Kuempel, C. D., Frazier, M., Blasco, G., Cottrell, R. S., Froehlich, H. E., et al. (2022). Mapping the spatial distribution of global mariculture production. *In Aquaculture* 553, 738066. doi: 10.1016/j.aquaculture.2022.738066

Coleman, S., Dewhurst, T., Fredriksson, D. W., St. Gelais, A. T., Cole, K. L., MacNicoll, M., et al. (2022a). Quantifying baseline costs and cataloging potential optimization strategies for kelp aquaculture carbon dioxide removal. *Front. Mar. Sci.* 9. doi: 10.3389/fmars.2022.966304

Coleman, S., St. Gelais, A. T., Fredriksson, D. W., Dewhurst, T., and Brady, D. C. (2022b). Identifying scaling pathways and research priorities for kelp aquaculture nurseries using a techno-economic modeling approach. In. *Front. Mar. Sci.* 9. doi: 10.3389/fmars.2022.894461

Costa-Pierce, B. A. (2016). Ocean foods ecosystems for planetary survival in the anthropocene. The Global Climate- Population Crisis. *World Nutr. Forum* 1, 301–320.

Costa-Pierce, B. A., Bockus, A. B., Buck, B. H., van den Burg, S. W. K., Chopin, T., Ferreira, J. G., et al. (2021). A fishy story promoting a false dichotomy to policy-makers: it is not freshwater vs. Marine aquaculture. In. *Rev. Fisheries Sci. Aquaculture* 1-18. doi: 10.1080/23308249.2021.2014175

Dean, R. G., and Dalrymple, R. A. (1991).

DNVGL. (2010). DNV-RP-C205. Environmental conditions and environmental loads. With assistance of Det Norske Veritas Germanische Llyod. 1st ed. C205. Hamburg, Germany: Det Norske Veritas Germanische Llyod (Environmental conditions and environmental loads). Available online at: http://www.dnvgl.com (accessed September 09, 2024).

Drew, B., Plummer, A. R., and Sahinkaya, M. N. (2009). A review of wave energy converter technology. *In Proc. Institution Mechanical Engineers Part A: J. Power Energy* 223, 887–902. doi: 10.1243/09576509JPE782

Eckert-Gallup, A. C., Sallaberry, C. J., Dallman, A. R., and Neary, V. S. (2016). Application of principal component analysis (PCA) and improved joint probability distributions to the inverse first-order reliability method (I-FORM) for predicting extreme sea states. *In Ocean Eng.* 112, 307–319. doi: 10.1016/j.oceaneng.2015.12.018

European Commission. Joint Research Centre. (2020). *Global warming and windstorm impacts in the EU: JRC PESETA IV project: Task 13* (Luxembourg: Publications Office of the European Union).

FAO. (2020). "Transforming food systems for affordable healthy diets," in *The state of food security and nutrition in the worl* (FAO, Rome).

Føre, H. M., Endresen, P. C., and Bjelland, H. V. (2022). Load coefficients and dimensions of raschel knitted netting materials in fish farms. *J. Offshore Mechanics Arctic Eng.* 144, 041301. doi: 10.1115/1.4053698

Fredriksson, D. W., DeCew, J., Swift, M., Tsukrov, I., Chambers, M. D., and Celikkol, B. (2004). The design and analysis of a four-cage grid mooring for open ocean aquaculture. *Aquacultural Eng.* 32, 77–94. doi: 10.1016/j.aquaeng.2004.05.001

Froehlich, H. E., Gentry, R. R., Lester, S. E., Rennick, M., Lemoine, H. R., Tapia-Lewin, S., et al. (2022). Piecing together the data of the U.S. marine aquaculture puzzle. *J. Environ. Manage.* 308, 114623. doi: 10.1016/j.jenvman.2022.114623

Froehlich, H. E., Smith, A., Gentry, R. R., and Halpern, B. S. (2017). Offshore aquaculture: I know it when I see it. *Front. Mar. Sci.* 4. doi: 10.3389/fmars.2017.00154

Gansel, L. C., Oppedal, F., Birkevold, J., and Tuene, S. A. (2018). Drag forces and deformation of aquaculture cages—Full-scale towing tests in the field. *In Aquacultural Eng.* 81, 46–56. doi: 10.1016/j.aquaeng.2018.02.001

Gansel, L. C., Plew, D. R., Endresen, P. C., Olsen, A. I., Misimi, E., Guenther, J., et al. (2015). Drag of clean and fouled net panels–measurements and parameterization of fouling. *PloS One* 10, e0131051. doi: 10.1371/journal.pone.0131051

Gentry, R. R., Froehlich, H. E., Grimm, D., Kareiva, P., Parke, M., Rust, M., et al. (2017). Mapping the global potential for marine aquaculture. *Nat. Ecol. Evol.* 1, 1317–1324. doi: 10.1038/s41559-017-0257-9

Gimpel, A., Stelzenmüller, V., Grote, B., Buck, B. H., Floeter, J., Núñez-Riboni, I., et al. (2015). A GIS modelling framework to evaluate marine spatial planning scenarios: Co-location of offshore wind farms and aquaculture in the German EEZ. *Mar. Policy* 55, 102–115. doi: 10.1016/j.marpol.2015.01.012

Goseberg, N., Chambers, M. D., Heasman, K., Fredriksson, D., Fredheim, A., and Schlurmann, T. (2017). "Technological approaches to longline- and cage-based aquaculture in open ocean environments," in *Aquaculture perspective of multi-use sites in the open ocean*. Eds. B. H. Buck and R. Langan (Springer International Publishing, Cham), 71–95.

Gray, L. (2019). Developing criteria and methodology for determining aquaculture zones under Marine Spatial Planning in the EU. *Recommendations MSP planners* 1, 1–43. Available at: https://aac-europe.org/images/AAC_-_Criteria_to_Locate_Aquaculture_-_Deliverable_2_-_Final_Draft.pdf.

Hagen, R., Plüß, A., Ihde, R., Freund, J., Dreier, N., Nehlsen, E., et al. (2021). An integrated marine data collection for the German Bight – Part 2: Tides, salinity, and wave, (1996–2015). *In Earth Syst. Sci. Data* 13, 2573–2594. doi: 10.5194/essd-13-2573-2021

Hannemann, O. (2022). OpenSeaMap. 0.1.23. Available online at: https://map.openseamap.org/ (Accessed July 7, 2022).

Heasman, K. G., Sclodnick, T., Goseberg, N., Scott, N., Chambers, M., Dewhurst, T., et al. (2024). Utilisation of the site assessment energy indices for aquaculture in exposed waters: biology, technology, operations and maintenance. *Front. Aquac.* 3. doi: 10.3389/faquc.2024.1427168

Heasman, K. G., Scott, N., Smeaton, M., Goseberg, N., Hildebrandt, A., Vitasovich, P., et al. (2021). New system design for the cultivation of extractive species at exposed sites - Part 1: System design, deployment and first response to high-energy environments. *In Appl. Ocean Res.* 110, 102603. doi: 10.1016/j.apor.2021.102603

Helsley, C. E. (Ed.) (1997). *Charting the Future of Ocean Farming. With assistance of University of Hawaii Sea Grant College Program. Open Ocean Aquaculture. Maui, Hawai, 23rd - 25th April. 1st ed. 1 volume* (Hawai: National Oceanic and Atmospheric Administration (Charting the Future of Ocean Farming). Available at: https://repository.library.noaa.gov/view/noaa/38659/noaa_38659_DS1.pdf#page=137.

Jin, S., Zheng, S., and Greaves, D. (2022). On the scalability of wave energy converters. *In Ocean Eng.* 243, 110212. doi: 10.1016/j.oceaneng.2021.110212

Kapetsky, J. M., Aguilar-Manjarrez, J., and Jenness, J. (2013). *Global assessment of potential for offshore mariculture development from a spatial perspective* (Rome: Food and Agriculture Organization of the United Nations (FAO fisheries and aquaculture technical paper, 2070-7010, 549).

Keulegan, G. H., and Carpenter, L. H. (1958). Forces on cylinders and plates in an oscillating fluid. *J. Res. Natl. Bur. Stan.* 60, 423. doi: 10.6028/JRES.060.043

Krause-Jensen, D., and Duarte, C. M. (2016). Substantial role of macroalgae in marine carbon sequestration. *Nat. Geosci* 9, 737–742. doi: 10.1038/ngeo2790

Landmann, J., Fröhling, L., Gieschen, R., Buck, B. H., Heasman, K., Scott, N., et al. (2021). New system design for the cultivation of extractive species at exposed sites - Part 2: Experimental modelling in waves and currents. *Appl. Ocean Res.* 113, 102749. doi: 10.1016/j.apor.2021.102749

Lewis, M., Neill, S. P., Robins, P., Hashemi, M. R., and Ward, S. (2017). Characteristics of the velocity profile at tidal-stream energy sites. *In Renewable Energy* 114, 258–272. doi: 10.1016/j.renene.2017.03.096

Longdill, P. C., Healy, T. R., and Black, K. P. (2008). An integrated GIS approach for sustainable aquaculture management area site selection. *In Ocean Coast. Manage.* 51, 612–624. doi: 10.1016/j.ocecoaman.2008.06.010

Loverich, G., and Forster, J. (2000). Advances in offshore cage design using spar buoys. *In Mar. Technol. Soc. J.* 34, 18–28. doi: 10.4031/MTSJ.34.1.3

Loverich, G. F., and Gace, L. (1997). "The Effect of Currents and Waves on Several Classes of Offshore Sea Cages. With assistance of O. S.T. OceanSparTechnologies." in *Charting the Future of Ocean Farming, vol. 1. With assistance of University of Hawaii Sea Grant College Program. Open Ocean Aquaculture. Maui, Hawai, 23rd - 25th April, 1st ed*, vol. 1 volume . Ed. C. E. Helsley (National Oceanic and Atmospheric Administration (Charting the Future of Ocean Farming, Hawai), 131–144. Available at: https://repository.library.noaa.gov/view/noaa/38659/noaa_38659_DS1.pdf#page=137.

Mackay, E., and de Hauteclocque, G. (2023). : Model-free environmental contours in higher dimensions. *Ocean Eng.* 273, 113959. doi: 10.1016/j.oceaneng.2023.113959

MacLeod, M. J., Hasan, M. R., Robb, D. H. F., and Mamun-Ur-Rashid, M. (2020). Quantifying greenhouse gas emissions from global aquaculture. *Sci. Rep.* 10, 11679. doi: 10.1038/s41598-020-68231-8

McCormick, M. E. (2010). *Ocean engineering mechanics* (With applications / Michael E. McCormic. Cambridge: Cambridge University Press).

Moe Føre, H., Thorvaldsen, T., Osmundsen, T. C., Asche, F., Tveteås, R., Fagertun, J. T., et al. (2022). Technological innovations promoting sustainable salmon (Salmo salar) aquaculture in Norway. *In Aquaculture Rep.* 24, 101115. doi: 10.1016/j.aqrep.2022.101115

Morison, J. R., Johnson, J. W., and Schaaf, S. A. (1950). The force exerted by surface waves on piles. *J. Petroleum Technol.* 2, 149–154. doi: 10.2118/950149-G

Nijdam, D., Rood, T., and Westhoek, H. (2012). The price of protein: Review of land use and carbon footprints from life cycle assessments of animal food products and their substitutes. *Food Policy* 37, 760–770. doi: 10.1016/j.foodpol.2012.08.002

Oyinlola, M. A., Reygondeau, G., Wabnitz, C. C. C., Troell, M., and Cheung, W. W. L. (2018). Global estimation of areas with suitable environmental conditions for mariculture species. *PloS One* 13, e0191086. doi: 10.1371/journal.pone.0191086

Poore, J., and Nemecek, T. (2018). Reducing food's environmental impacts through producers and consumers. *Sci. (New York N.Y.)* 360, 987–992. doi: 10.1126/science.aaq0216

Przedrzymirska, J., Zaucha, J., Calado, H., Lukic, I., Bocci, M., Ramieri, E., et al. (2021). Multi-use of the sea as a sustainable development instrument in five EU sea basins. *In Sustainability* 13, 8159. doi: 10.3390/su13158159

QGIS Development Team. (2022). *Quantum GIS. Version long term release (LTR) 3.16.16. Open source geospatial foundation project* (Beverton, Oregon, United States). Available at: http://qgis.osgeo.org.

Sarpkaya, T. (2014). *Wave forces on offshore structures* (Shaftesbury Road Cambridge: Cambridge University Press).

Schupp, M. F., Bocci, M., Depellegrin, D., Kafas, A., Kyriazi, Z., Lukic, I., et al. (2019). Toward a common understanding of ocean multi-use. *Front. Mar. Sci.* 6. doi: 10.3389/fmars.2019.00165

Stevens, C., Plew, D., Hartstein, N., and Fredriksson, D. (2008). The physics of open-water shellfish aquaculture. *Aquacultural Eng.* 38, 145–160. doi: 10.1016/j.aquaeng.2008.01.006

Sulaiman, O. O., and Abdul Raship, A. R. N. B. (2013). Macro algae: biodiversity, usefulness to humans and spatial study for site selection in oceanic farming. *J. Biodivers Endanger Species* 01, 1-6. doi: 10.4172/2167-1206.S1-003

The Mathworks Inc. (2022). *Matrix laboratory (MatLab). R2020a, update 7. Version 9.8.0.1721703* (Natick, Massachusetts: The Mathworks Inc). Available at: www.matlab.com.

Tilman, D., Balzer, C., Hill, J., and Befort, B. L. (2011). Global food demand and the sustainable intensification of agriculture. *Proc. Natl. Acad. Sci. United States America* 108, 20260–20264. doi: 10.1073/pnas.1116437108

Tsukrov, I., Drach, A., DeCew, J., Robinson Swift, M., and Celikkol, B. (2011). Characterization of geometry and normal drag coefficients of copper nets. *In Ocean Eng.* 38, 1979–1988. doi: 10.1016/j.oceaneng.2011.09.019

United Nations. (2020). *SUSTAINABLE DEVELOPMENT GOALS REPORT 2020. With assistance of UN-DESA, UNITED NATIONS DEPARTMENT FOR ECONOMIC AND SOCIAL AFFAIRS* (New York, NY, United States: United Nations Publication).

United Nations. (2022). World Population Prospects 2022. Summary of Results. With assistance of UN-DESA, UNITED NATIONS DEPARTMENT FOR ECONOMIC AND SOCIAL AFFAIRS. Available online at: https://www.un.org/development/desa/pd/sites/www.un.org.development.desa.pd/files/wpp2022_summary_of_results.pdf (Accessed July 5, 2022).

USACE. (2002). *Coastal Engineering Manual. Water Wave Mechanics. EM 1110-2-1100. With assistance of United States Army Corps of Engineers. 2nd ed* Vol. 5 (Washington, USA: US Army). Available at: https://pdf.js/ccc3e492-f3d7-4763-803a-2e0090f188b4#filename=EM_1110-2-1100_Ch_01.pdf.

van Vliet, J., de Groot, H. L., Rietveld, P., and Verburg, P. H. (2015). Manifestations and underlying drivers of agricultural land use change in Europe. *Landscape Urban Plann.* 133, 24–36. doi: 10.1016/j.landurbplan.2014.09.001

Welzel, M., Schendel, A., and Goseberg, N. (2021). GWK +: Erweiterung des Großen Wellenkanals – Analyse des Einlaufbereichs. *Bautechnik* 98, 541–551. doi: 10.1002/bate.202100042

Winkler, K., Fuchs, R., Rounsevell, M., and Herold, M. (2021). Global land use changes are four times greater than previously estimated. *In Nat. Commun.* 12, 2501. doi: 10.1038/s41467-021-22702-2

Zhan, J. M., Jia, X. P., Li, Y. S., Sun, M. G., Guo, G. X., and Hu, Y. Z. (2006). Analytical and experimental investigation of drag on nets of fish cages. *In Aquacultural Eng.* 35, 91–101. doi: 10.1016/j.aquaeng.2005.08.013

Zuzak, C., Goodenough, E., Stanton, C., Mowrer, M., Ranalli, N., Kealey, D., et al. (2021). *National risk index. Technical documentation* (Washington, DC, USA: Fderal Emergency Management Agency). Available at: https://www.fema.gov/sites/default/files/documents/fema_national-risk-index_technical-documentation.pdf.